8-2022

Rotational Spectroscopy of Nonafluoro-tert-butyl Alcohol

Zayra Leticia Gonzalez
The University of Texas Rio Grande Valley

ROTATIONAL SPECTROSCOPY OF NONAFLUORO-TERT-BUTYL ALCOHOL

A Thesis

by

ZAYRA LETICIA GONZALEZ

Submitted in Partial Fulfillment of the

Requirements for the Degree of

MASTER OF SCIENCE

Major Subject: Chemistry

The University of Texas Rio Grande Valley

August 2022

ROTATIONAL SPECTROSCOPY OF NONAFLUUORO-

TERT-BUTYL ALCOHOL

A Thesis
by
ZAYRA LETICIA GONZALEZ

COMMITTEE MEMBERS

Dr. Wei Lin
Chair of Committee

Dr. Shervin Fatehi
Committee Member

Dr. Erik Plata
Committee Member

Dr. Javier Macossay-Torres
Committee Member

Dr. Manar Shoshani
Committee Member

August 2022

ABSTRACT

Gonzalez, Zayra L., The Rotational Spectroscopy of Nonafluoro-tert-butyl alcohol. Master of Science (MS), August, 2022, 92 pp., 6 tables, 22 figures, references, 131 titles.

Nonafluoro-tert-butyl alcohol (NFTBA) is an alcohol being used in medicine and for the analysis of physiochemical and biological properties. Quantum chemical calculations on NFTBA were carried out using cluster computers from the Texas Advanced Computing Center (TACC) at Austin, TX. We scanned the C–C–O–H dihedral angle for 36 steps with each step at 10 degrees at the B3LYP/aug-cc-pVTZ level in order to identify the stable conformations and the energy barriers. The geometry of nonafluoro-tert-butyl was studied using MP2 and B3LYP Density Functional Theory (DFT) with an aug-cc- pVTZ basis set. The calculated rotational constants and dipole moments were used to help interpretation of the experimental study of nonafluoro-tert-butyl alcohol using microwave spectroscopy. We anticipate that large amplitude motions would occur on the alcohol group which may further perturb its rotational spectrum. The measured spectrum shows a very strong intensity of rotational transitions.

DEDICATION

I would like to dedicate this thesis to the most important person in my life who has been there for me from the very start to God, my lord, and Savior Jesus Christ whom I would not be here today. I will love to dedicate this thesis and the hard work on writing to those who have pushed me to continue my education and guided me in my time studying chemistry. To my mother, Bertha Lilia Gonzalez, and to my father, Javier Gonzalez Garcia, with all their sacrifices done to help me in continuing my education. I would not be doing this without them and for being my biggest cheerleaders and supporters in working hard in my education; I would not have been here without you two I love you. Also, to the person who is not here with my today my brother Carlos Alberto Gonzalez who passed away at a young age of 10 who is the reason that I pushed myself to do my best and for me to be studying I miss you, but I know you are watching me from where you are and always cheering for me in my goals.

I would like to thank my family for being my supporters and for being there for me to do my best you are always there for me. To my best friends l also like to dedicate this to my best friends who have supported me and being there for me I would not have been here without your support and always being there with me and pushing me to study having all-nighters. To my mentor Dr. Wei Lin who has been a great supporter and been an amazing mentor that has been a supporter in succeed and teaching me when I have questions. Dr. Lin's research group Michael, Diego, Karla, Alitza, Amanda, and Keila for being the most amazing friends I have made and being there to make me learn you guys have been the biggest support I have had.

ACKNOWLEDGMENTS

I want to acknowledge the following people who have pushed me to work hard and not give up on writing this thesis. I want to thank God, who has been my sail in these moments of writing this thesis and giving me the knowledge and strength to keep going in my master's. My parents have been my most extensive support in all this work on my idea and have been my cheerleaders and motivators to keep going when I had sleepless nights studying and working on exams and being late at the library at night. My family, grandmother, aunts, uncles, and cousins have been supportive in this phase in my life. My friends have also been supportive of this study for my thesis. I want to acknowledge my high school chemistry teacher, Mr. Lanaghan. He was the one that made me like chemistry a lot and motivated me to see that science is around us. I give him much gratitude because it inspired me to enter my degree in chemistry. Also, the scientist who pioneered and whom I looked up to made me love science Isaac Newton, Galileo Galilei, Marie Curie, Jane Marcet, Lous Pasteur, Alfred Nobel, Rosalind Franklin, Albert Einstein, Irene Joliot-Curie, and many more. They inspired me to be in this profession in science and my degree in chemistry. To my professors who have taught me through my undergraduate and graduate courses, thank you for all you have taught me to understand and be able to work hard Dr. Plata (Ochem), Dr. Shizue Mito (Special Topics Ochem), Dr, Macossay (Adv. Ochem, Grad Ochem elective), Dr. Jason Parsons (Analytical, Inorganic, Instrumental, Chem Problems, and Environmental) Dr. Evangelia Kotsikorou (Pchem Graduate pchem and Physical BioChem) Dr. Tulay Atesin (Advance Inorganic), Dr. Abduharrahman Atesin (Grad Inorganic).

At the same time, I want to give my gratitude and acknowledgment to my undergraduate and graduate mentor, Dr. Wei Lin. I am very grateful for all the support, mentoring, guidance, knowledge, and care that you have shown from making me into your research lab as an undergraduate and now as a graduate student. I learned so much from you; however, the pandemic did cause much disruption in the research plans, but we kept working.

I look forward to keeping in contact with you as I am in a new chapter in my chemical career. I am also grateful to Dr. Lin's research group, the kindest and most supportive group. Michael Carrillo, Karla Salazar, Diego Rodriguez, Alitza Gracia, Keila Murillo, and Amanda Torres. Finally, Dr. Grubbs and his research group, such as his students Joshua Isert, from the Missouri Science and Technology University, who collaborated on this investigation and had as much interest in what we were studying on as we were.

TABLE OF CONTENTS

Page

ABSTRACT iii
DEDICATION iv
ACKNOWLEDGMENTS v
TABLE OF CONTENTS vii
LIST OF TABLES ix
LIST OF FIGURES x
CHAPTER I. INTRODUCTION TO NONAFLUORO-TERT-BUTYL ALCOHOL 1
1.1 Introduction 1
1.2. Chemistry of Fluorine 3
1.3 Tert-Butyl and 2,2,2-Trifluoromethanol Alcohol 8
1.4 Research on Nonafluoro-Tert-Butyl Alcohol 15
CHAPTER II. COMPUTATIONAL WORK 17
2.1 Schrödinger Equation 17
2.2 Methods 22
2.2.1 Density Functional Theory 25
2.2.2 Second-Order Møller Plesset Perturbation Theory 28
2.3 Basis Sets 30
2.4 Hardware 33
2.5 Software 35
2.5.1 Gaussian 35
2.5.2 Pgopher 37
CHAPTER III. ROTATIONAL SPECTROSCOPY 38
3.1 Introduction of Rotational Spectroscopy 38
3.2 Principles of Rotational Spectroscopy 42
3.3 Rigid Rotor 50
3.4 Centrifugal Distortion Constant 56
3.5 Large Amplitude Motions 60
3.6 CP-FTMW Spectrometer 62

CHAPTER IV. ROTATIONAL SPECTROSCOPY NONAFLUORO-TERT-BUTYL ALCOHOL 65
4.1 Theoretical Work 65
4.2 Experimental work 70
4.3 Summary 79
REFERENCES 80
BIOGRAPHICAL SKETCH 92

LIST OF TABLES

Page

Table 3. 1:The four different types of Geometric structures of rigid rotors 43
Table 3. 2: The Angular and linear motion relation 45
Table 4. 1:Energy barriers comparison of NFTBA with TBA 67
Table 4. 2:Structural Parameters of NFTBA 68
Table 4. 3: Calculations of NFTBA 72
Table 4. 4:Preliminary Fitting MS&T and UTRGV 77

LIST OF FIGURES

Page

Figure 1. 1:Fluorspar (CaF6) 4
Figure 1. 2: Atomic bomb replicas of Little Boy and Fat man made with Uranium 5
Figure 1. 3: Fluorine dangers to Ozone 6
Figure 1. 4: Fluorination effect from TBA to NFTBA 8
Figure 1. 5:TFA and NFTBA 11
Figure 2. 1:Seymour Cray with his Cray-1 Supercomputer 34
Figure 2. 2: Pople Diagram of Basis set for Gaussians software for atomic orbitals 36
Figure 3. 1: Electromagnetic Spectrum 40
Figure 3. 2: Circular motion 44
Figure 3. 3: Spherical molecule rotor 46
Figure 3. 4:Oblate and Prolate molecule rotors 47
Figure 3. 5: Asymmetric top selection rules 49
Figure 3. 6: Rigid Rotor model 50
Figure 3. 7: Diatomic/ Linear Molecule selection rule 54
Figure 3. 8: Centrifugal distortion constant describing the stretching motion 57
Figure 3. 9: Centrifugal distortion constant effect 58
Figure 3. 10: CP-FTMW Spectrometer schematic 63
Figure 4. 1: Potential Energy Scan for Nonafluoro-tert-butyl alcohol conformation along with dihedral angle τC1-C2-O14-H15 66
Figure 4. 2: Calculated structure of NFTBA 70
Figure 4. 3: Simulated calculation Nonafluoro-tert-butyl alcohol 73
Figure 4. 4: Rotational Spectrum Nonafluoro-tert-butyl alcohol 75
Figure 4. 5: Comparison of experimental (bottom) and simulated *c* type transitions (up) of nonafluoro-tert-butyl alcohol (6 -10 GHz) 76

CHAPTER I

INTRODUCTION TO NONAFLUORO-TERT-BUTYL ALCOHOL

1.1 Introduction

Nonafluoro-tert-butyl alcohol (NFTBA) has been studied worldwide, including in the United Kingdom, Japan, Canada, and the United States. It has been used in various fields such as pharmaceutical, organic, polymer, biomedical, and biological applications. NFTBA has only been researched in the synthesis reaction since the start of the 1960s due to being a per halogenated alcohol by its high acidity (Pavlick 1970). Nonafluoro-tert-butyl alcohol (NFTBA) has been investigated for its magnetic resonance properties, and for the effects fluorine brings in the molecules by substituting hydrogens (Wu, 2021). The alcohol has a pKa of 5.2 (Han, 2020). The fluorination effect makes it more acidic and therefore more miscible in water. NFTBA is highly irritant, corrosive, and cancerogenic; protective wear is typically required when used by a person. (Filler, 1967). NFTBA has been used as a reagent in forming a polymer (Decanto, 2014) for biological electron reduction on drugs for cancer tumors. Experimental spectroscopy investigations on medicinal drugs and pharmaceutical testing (Cabaço, 2021). The NFTBA has been used to calculate how it works with its heterodimers on the organic chemistry analysis of its stabilization energies. These halogenated alcohols have sparked interest in how fluorine interacts with the molecule based on magnetic resonance (Cabaço 2021).

To our best knowledge, this project is the first report on the rotational spectroscopy of this molecule. We are looking at the different characteristics of fluorine by its reactions and interactions within the atoms in the molecule. We studied the conformational landscape of NFTBA to understand the fluorination effect better.

1.2 Chemistry of Fluorine

There is so much interest today in fluorine chemistry, what it does to the bonds in the compounds, materials, and what reactions it makes. Fluorine was used by many in the 16th century by Georgius Agricola, a natural halide mineral such as fluorspar or fluorite (CaF_2)(Roesky 2010); this is used for glass and steel making since it's durable for many uses today; in the 17th century it was used with glass as fluorspar and when it was treated with acid it started to cause a reaction such as corrosion, a Swedish chemist and pharmacist, Carl Wilhelm Scheele, found hydrofluoric acid in 1771 (Pubchem 2004). Fluorine is a halogen that has been mentioned since the 18th century when this atom was found on the earth. However, the isolated fluorine was not discovered until the 19th century by French chemist Henry Moissan as a liquid solution. He found that it was in a solution of potassium bifluoride (KHF_2), which is an anhydrous solution from hydrofluoric acid (HF), and he received the Nobel prize for chemistry in 1906 (Roesky 2010). This discovery led to an extensive work of finding the fluorination effect and what this can do in many areas of science. This topic of investigation has been over 70 years since fluorine was used for many experiments; however, it was not until the 1970s that it started to become a topic for article publication due to its popularity in various project analyses. These interests have been explained in the previous sections and used in different areas of science such as chemistry, medicine, industry, materials, polymers, geology, and biology for the past few centuries. For example, fluorine is increasing in popularity for its many characteristics and unique formation in the material for the earth, like in figure 1.1 of fluorspar.

Figure 1. 1:Fluorspar (CaF6)

Physical properties and uses of fluorite. Physical Properties and Uses of Fluorite_Chemicalbook. (2009, December 3). Retrieved February 18, 2022, from https://www.chemicalbook.com/Article/Physical-Properties-and-Uses-of-Fluorite.htm

The paramount importance of this project is to understand fluorine to open up on what other ways fluorine can be helpful today. The fluorine in its magnetic resonance is based on its wide range by the chemical shifts the fluorine makes within the molecule (Gouverneur 2015). The fluorination effect has been noticed in medicine with NMR and UV light studies in looking at how fluorine has a significant advantage in its use in science. Its studies show unique physiochemical properties that give some design to the mechanism in many biochemical or polymerized products. For example, studies have shown how good fluorine has been studied for its use in medical drugs for cancer tumors and has been tested, such as using two polymers that are hydrophilic and have fluorine polymers in their injections (Jirak 2018). That study has shown that it has been a great use of this polymer with fluorine. Still, it can also be biodegradable, and notice its significant effects on the tumors when studied and trying to find a way it won't leave any biodegradable residue in the body by having fluorine part of the polymers (Jirak 2018). There is much to understand on how much this atom can do for many compounds on its effects

physiochemically. Other than polymers, fluorine is used in the creation of pharmaceuticals. Fluorine has had a significant impact on medicine and using a proportionate amount of fluorine. This is based on how fluorine has a substantial, influential role in medicinal chemistry by creating fluorinated steroids (Hagmann 2008) and fluorinated anesthesia, like fluoroxene, causing problems in the ozone to fluoro-ethers in the 1950s (Molina 1974).

Figure 1. 2: Atomic bomb replicas of Little Boy and Fat man made with Uranium

Griffith, C., & Rossenfeld, C. (n.d.). *Little Boy & Fat Man*. National Museum of Nuclear Science & History | Photographs | Media Gallery. Retrieved May 1, 2022, from https://www.atomicarchive.com/media/photographs/nuclear-journeys/nmnsh/nmnsh-12.html

Also, fluorine has been used to characterize its fluoropolymers by creating Teflon for cooking pans, which was discovered by Roy Plunkett in the late 1930s, as seen in its use in the industrial world (Wakselman 1994). The use of fluorine has opened an abundant source of organofluorine chemistry for commerce for many polymers since it's also been liquified for

many graphics and computer useage (Scheirs 1997). There have also been studies on how fluorination effect organic compounds by changing properties in semiconductors (Jiang 2019). In this experiment with the addition of fluorine, it was noticed that it caused a change in the geometry, including its molecular orbitals. Detecting the pi electrons within the organic molecule in the solid state is also shown in its gas phase when it's being calculated computationally.

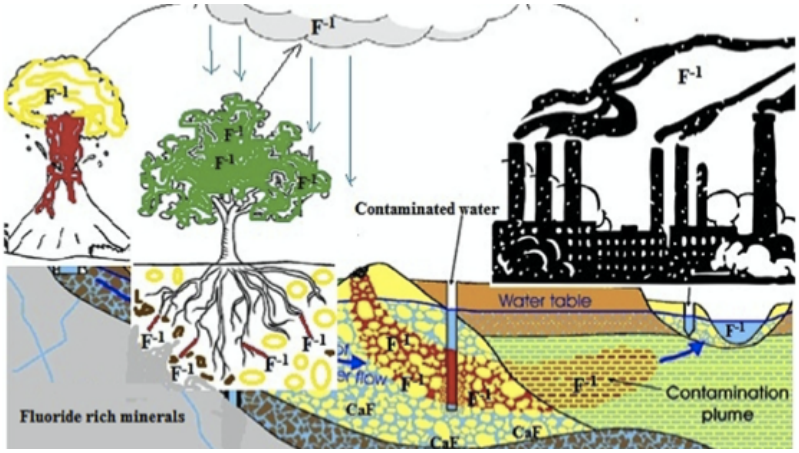

Figure 1. 3: Fluorine dangers to Ozone

Singh, G., Kumari, B., Sinam, G., Kriti, Kumar, N., & Mallick, S. (2018). Fluoride distribution and contamination in the water, soil and plants continuum and its remedial technologies, an Indian perspective– A Review. *Environmental Pollution*, *239*, 95–108. https://doi.org/10.1016/j.envpol.2018.04.002

Research with fluorine today has not stopped in the investigation process of the use of fluorine for many operations of materials. It has become a popular halogen for many scientific projects and analyses. It has also become a hazardous effect on the ozone by pollution—the dangers of using fluorine since it is a very toxic gas. During World War II during the 1940s, in Germany, chlorine trifluoride was manufactured for the creation of atomic bombs by the Oberkommando des Heeres (Dinoui 2006). Then the United States had a vast production of fluorine; the Manhattan project used fluorine to create uranium hexafluoride (UF6), which was

used to separate the ^{235}U and ^{238}U isotopes of uranium. These were used with fluorine and uranium; it made this Uranium isotope was used as bombs for Nagasaki and Hiroshima in Japan, causing radiation. The use of fluorine has become popular in how it can also be great when creating alcohols into very acidic changing everything of its This is how this fluorine makes any effects that can cause it to be an essential source, and by looking at how fluorine can make this reaction, what does it do to the other atoms in this compound, and what else does it create some reaction.

1.3 Tert-Butyl and 2,2,2-Trifluoroethanol Alcohol

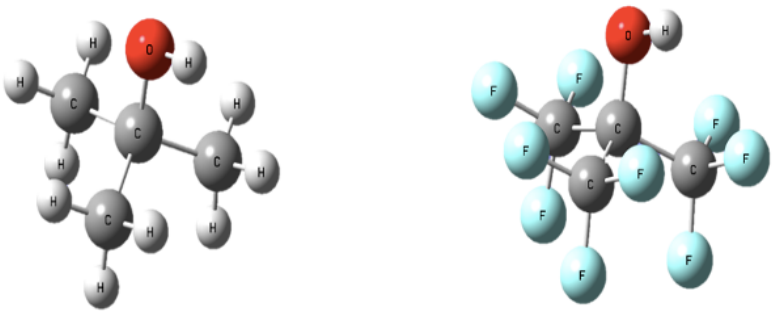

Figure 1. 4: Fluorination effect from TBA to NFTBA

The use of tert-butyl alcohol (TBA) has been a significant source of information in the literature reviews of molecules close to NFTBA. TBA's data information has some similar foundation that helped in my research in computational and experimental with NFTBA. This molecule literature review paper provides a template for my research on what similarities it has and what won't be identical in data. The TBA and NFTBA are both from the same root. Their interactions with the fluorine molecule have brought more acidity based on different interactions of hydrogens with the tert-butyl alcohol. They come from the same root, but it shows how they differ based on their pKa and resonance. Also, how they differ in the research used for research opens the opportunity for TBA to expand when having halogens and makes scientists interested in how they change the molecule.

Tert-butyl alcohol was studied for rotational spectroscopy by Dr. E. A. Valenzuela for his Ph.D. thesis between 1974 and 1975 with Dr. R. C. Woods using the A and E state transitions from the R-branch transition. He was studying its first rotational spectrum by undergoing the experiment using computational work based on its dipole moments and by using a program to

use a basis set for their calculations which they noticed the interaction between the values (A+B) and how they were the only values that could be seen in the spectrum using the program RHOBAS (Valenzuela 1975). This led to the 8–40 GHz region showing over two hundred lines over the Stark effect of the weak impact to determine the exact number based on the values of rotational levels to locate the transition in the microwave spectrum. Tert-butyl alcohol analysis provided the transition of perpendicular and parallel transitions; however, the *C((A-B)/2)*, *A-B*, and β could not be observed in the low energy parameter experiment. Although in the double resonance experiments, they could see these values and get about 70 transitions from only the E-level transitions getting the fits of the Hamiltonian nine parameters. After this research from Dr. Valenzuela had made on tert-butyl alcohol in 2010, there was a following study based on the values that were done in the first experiment by the participation of Dr. E. A. Cohen. This rotational spectrum of tert-butyl alcohol was by using the early data from the University of Wisconsin from the 8-40 GHz region and then combining the newest measurements by using the spectrums of 8- 500 GHz done from the university of bologna and the Jet Propulsion Laboratory (JPL) from the millimeters and submillimeter wavelength region (Cohen 2010). It can see in this study that other than the tert-butyl alcohol being an asymmetric top and a nearly spherical top based on the internal rotational axis from the *c*- molecular axis in the *ac* plane, from this continuation of the study, they were able to see some torsion within their spectrum done. The study showed how TBA was researched using the MP2, Second-Order Møller–Plesset perturbation theory, the basis sets 6-311++G and the program used for the single set molecular parameters from Pickett SPFIT (Pickett 1991) from Jet Pulsion Laboratory (JPL) for the quantum numbers of the experimental range of both the A and E internal rotation states.

We could now focus on how tert-butyl alcohol interacts within being in a liquid form and with other molecules. In studies they were made were based on the tert-butyl alcohol based on its function of pressure and temperature on how its simulation demonstrated a cyclic tetramer within its liquid structure and its pressure dependence was consistent, and its temperature can have some shift within the distribution and the stability of the hydrogen bonding (Yonker 1997). This was based on its other conformer being in a cyclic position to determine that it was the structure of the liquid as it was studied in NMR. In the rotational study of the molecular isotopologue, tert-butyl alcohol was used with 1,4-dioxane using a pulsed jet Fourier Transform microwave spectrometer to see interaction within its conformers and rotational constants (Evangelisti 2011). This research was done in Bologna, Italy, by Dr. Luca Evangelisti and Walther Caminati. They used the Gaussian 03 program, and ab initio calculations were done using method MP2 and basis set 6-311++G, including the SPFIT program (Pickett 1991). This was to see the stability of the hydrogen bond from the structure of the axial and the equatorial forms. They had to use a deuterated effect to interact with the proton and hydrogen bond within the tertbutyl alcohol and 1,4-dioxane.

Based on the rotational constants B and C being able to see on a large scale, the OH species could not reproduce in the inversion of size and were able to convey that they had stability in the axial form. The following study was done by Dr. Spada and his collaborators on the interaction of the 1:1 complex of tert-butyl alcohol with difluoromethane based on the potential energy of three stable isomer formations (Spada 2017). Based on the computational data from one isomer, the OH—F, and the two C-H—O weak hydrogen bonds based on the low interconversion barriers. In this study, they were able to see from within the bonding energy had increased from the hydrogen bonds some dissociation to be able to determine a “pseudo-diatomic

approximation," and that contributed to the isomers M1 being able to be seen based on its global minimum stability on the rotational spectra. The computational calculations used were Gaussian and Couples-Cluster for Computational Chemistry (CFOUR) (Mathews 2020) using the Tres Grande Centre de Calcul (TGCC) supercomputer in Europe using MP2, Hartree Fock (HF), DFT, and Couples Cluster Theory (CCSF(T)) with basis set of m-aug-cc-pVTZ minimal, and CBS for their calculations.

Figure 1. 5:TFA and NFTBA

2,2,2-Trifluoroethanol (TFA) is using another molecule to understand the work done in rotational spectroscopy and the interaction between the fluorine and the alcohol within the carbon bonds. Dr. Javix Thomas studied with his collaborators on the rotational spectroscopy of 2,2,2-trifluoroethanol trimers of its three stable conformers (I, II, and III) using the Fourier transform microwave spectrometer using the *ab initio* calculations (Thomas 2017). This study used the MP2, B3LYP-D3BJ and basis set 6-311++G, then the Gaussian09 and a multifunctional wavefunction analyzer (Multiwfn) program (Lu 2011) by performing QTAIM and NCI analysis. The trans-TFE was unstable in conformer I on its gas phase; however, the liquid phase of the TFE trans conformation is stable of clusters size incrementation from the gauche (+/-), and trans

conformers stability in the liquid face and showing that the TFE trimer is unstable also from the FTMW spectroscopy using 2–6GHz to be able to detect the H bonding and being seen. The investigation indicates that the O-H–O-H and the OH–F-C hydrogen bond has an attractive interaction and stabilizes the three conformers. Conformers I and III showed to be the main stabilizing driving forces.

They were also providing of the gauche-TFE subunit of the exchange within the C–F—— F–C pairs in contact and the three points of F–F–F attractive contact interaction within the TFE clusters. Other studies being done with TFE had been with other molecules such as water and ammonia complex by Dr. Thomas and collaborators. The analysis of the structure and tunneling modeling between TFE and water complex based on the hydrogen bonding and the tunneling dynamics using conformers of TFE looking at the intramolecular hydrogen bond (Thomas 2014). In this study, they were able to see the bonding and nonbonding hydrogen atoms in the water causing an absence of splitting in the rotational transition from what was observed and add the splitting on the rotational transition indicating the tunning from g+ and g- of TFE when quenching within the TFE and H_2O complex. In this research, Jet cooled FT microwave spectroscopy, and the basis set they used was 6-311++G, and the method was MP2. Overall, the rotational spectra of these solvents with TFE and water complex allowed them to see tunneling splitting of the rotational transition with two and nuclear statistical analysis based on the bonded and nonbonded hydrogen atoms of the water. The tunning was between the g+ and g- of the TFE, mainly since it forms an insertion rather than making an addition complex with water. The TFE and ammonia complex was investigated using the Chirped pulse, cavity-based Fourier transform microwave spectroscopy, and computational methods of the stability within the gauche TFE and NH_3 conformer within the intramolecular hydrogen bonds (Thomas 2020). Also, the ammonia

indicated free internal rotation by showing the stabilization within the primary OH-N hydrogen bond and secondary N–H–F interaction and having internal dynamic effects found in the rotational spectra. The significant amplitude motion showed the tunneling in the rotational spectra of the stabilization of the two intermolecular gauche configurations of the OH-N and NH-F and one intramolecular OH-F. The gauche g+ and g- of the TFE are quenched by the hydrogen-bond interaction with ammonia. Also, the theoretical calculation showed the agreement within the experimental B and C rotational constants.

Although Trifluoroethanol is not similar in its molecular structure, it is like nonafluoro-tert-butyl alcohol. This could have some information that could be helpful to use in my research to have something that can be used when working on my research.

As we have learned from the molecules similar to nonafluoro-tert-butyl alcohol, now we focus on the molecule that is precisely the same as nonafluoro-tert-butyl alcohol being perfluoro-tert-butyl alcohol (PFTBA) which there was an article based on the large amplitude of motion. There was a study by Dr. Yokoszeki and his collaborator in 1974 that studied the sample of perfluoro-tert-butyl alcohol that was from the Penninsular ChemResearch, seeing electron diffraction patterns from the room temperature based on the distance that was not in harmony with the distances by the tert-butyl compounds. The large amplitude of motion of the electron diffraction intensity from the PFTBA gas phase is based on the motion of multiple rotors from the three CF_3 and one OH, which was studied in the balance from the nonbonded interactions from F–F, C–F, and O–F pairs (Yokozeki 1974). From what was seen, some contributed torsional motions from the electron diffraction of motion with multiparameter large amplitude motion based on the nonbonded interactions from F–F pair causing twisted staggered positions. They had to use the Monte Carlo methods (Hammersley 1965) to be based on seeing the motion

of the CF_3, and based on the evaluation, they were able to produce the integrals evaluating by the appearance that there is multiparameter large amplitude motion of the electron diffraction analysis.

1.4 Research on Nonafluoro-Tert-Butyl Alcohol

In chapter 4, we will focus on the work that was done based on geometry optimization and potential energy scan. This will be focused on the work done on theoretical and then experimental work. Including we will be able to explain further why we did this theoretical work and its importance in our study from the focus on our alcohol in the interaction it has with the fluorine-based on what we are analyzing in this overall thesis. In comparing the data, we have gotten from the energy barriers with the TBA and 2,2,22-trifluoroethanol. This we can also talk about comparing them could give an insight on how we have an interest in the fluorination effect and including the alcohol on why it provides a large amplitude motion regarding our molecule. Based on our collaboration, we could also go further on how we could see that our molecule being an asymmetric molecule, can be a nearly oblate molecule.

However, further chapters are based on the NFTBA studies used to perform the computational work, the rotational spectroscopy, and why they are essential in this research. We will learn about the computational work done with the methods of Density functional theory (DFT) and (MP2) Second-Order Moller Plesset Theory. Also, the basis set 6-311++G and aug-cc-pVTZ and the programs that had been used Pgopher for the rotational spectra of NFTBA and Gaussian to make our molecule NFTBA. Then, to conduct a computational experiment, we used Texas Advanced Computer Center (TACC) to send our work to be calculated and scanned. Then we worked on using the Chirped-Pulse Fourier transformed Microwave Spectrum to do our experimental work. We collaborated with Dr. Garry “Smitty” Grubbs and his research group from the Missouri University of Science and Technology. After, we will talk about what was seen in this investigation that had been done overall from this study, understanding what went through the rest of the scan and the rotational spectroscopy based on the analysis done from the

computational work to the experimental based on this experiment to be able to do more studies in this research.

Furthermore, we hope to our study's primary interest and broaden the opportunity from our research of NFTBA. We can analyze this study more in-depth and expand the investigation with this alcohol shortly.

CHAPTER II

COMPUTATIONAL WORK

2.1 Schrödinger Equation

Quantum physics started from Newtonian mechanics, which pushed for molecular and atomic work studies from the late nineteen century to understand electromagnetic behavior from molecules and atoms (McQuarrie 1997). Isaac Newton's law of motion could be used to represent classical motion accurately, as shown in Newton's second law equation (2.1)

$$F = ma \qquad (2.1)$$

This equation is fundamental to classical mechanics because it can depict the motion of a ball rolling in the field and then hitting another. Since electrons are very light particles and cannot be described in classical mechanics. The Schrödinger equation is a fundamental quantum mechanics since it is based on the solution of the wave functions theorized since the 1920s. The Schrödinger equation is based on how time is not a variable making it time-independent and a stationary wave function. The formula in the Schrödinger equation is to solve the particle-wave of matter and wave functions. The Schrödinger equation derives from the Newtown formula and the Broglie to get a derivative from then to get time out from the solution. Time-dependent equation is used to describe the change in the system over time, and time-independent equation depends on the

position of a particle that is independent of time. The mechanical equation corresponds to Newton's second law is the time-independent Schrödinger equation (Schrödinger 1926) 2.2.

$$-\frac{\hbar^2}{2m}\frac{d^2}{dx^2}\psi(x) + V(x)\psi(x) = E\psi(x) \tag{2.2}$$

In Equation 2.2 differential equation solution *ψ(x)* described particle of a mass *m,* moving in a the 1D field described *V(x)* according in to the wavefunction $\psi(x)$ with energy *E*. The time-independent Schrödinger equation 2.3 represents it corresponds to the particle's different stationary states, giving a non-relativistic description of the system.

$$\hat{H}\Psi = E\Psi \tag{2.3}$$

The $\hat{H}$, is the Hamiltonian operator, and E is the energy of the wave function, Ψ, of the molecule or the atoms. In Schrödinger's equation, the solution was to use them based on the Hamiltonian operator equation using the energy from an eigenvalue based on the wavefunctions since it does not depend on time. Thus, physicists and chemists used the simplistic formula to calculate using the Hamiltonian equation. The Schrödinger Equation focused on adapting based on describing the interaction between mutual particles (von Neumann 1929). The Schrödinger equation is for the advancement into understanding the wavefunction particles of the molecules and changing to a more based on the constant operation of the eigenfunctions for linear momentum. The Hamiltonian Operator was used to solve the molecular interaction of the compound atoms based on its potential and kinetic energy (Jensen 1999) using equation (2.3).

The Hamiltonian operator equation used for Schrödinger's equation for a molecular system involves a kinetic and potential energy part, as shown in equation 2.4.

$$H = T + V \tag{2.4}$$

The kinetic energy, T, by using the kinetic operator using particle its derivation by using Laplacian for the overall summation in equation (2.5)

$$T = -\frac{\hbar^2}{2}\sum_{i}\left(\frac{1}{m_i}\left(\frac{\partial^2}{\partial x_i^2}+\frac{\partial^2}{\partial y_i^2}+\frac{\partial^2}{\partial z_i^2}\right)\right) = -\frac{\hbar^2}{2}\sum_{A}^{N}\frac{1}{M_A}\nabla_A^2 - \frac{\hbar^2}{2}\sum_{i}^{n}\frac{1}{m_i}\nabla_i^2 \tag{2.5}$$

In equation 2.5, the first two terms represent the kinetic energy from the nuclei and electron, as the other four equations consider the potential energy. The third equation is what takes the nuclear-electron attraction, and the last two equations, the fourth and fifth, carry the potential energy force repulsion that is going through the electrons and the nuclei. This is based on deriving the Hamiltonian operator of the molecular orbital analysis. The approximation has to be applied to the reduction of the dimension of this function by derivation to simplify the equation to a smaller product by the end by giving the problem in equation 2.6.

$$\mathrm{H} = -\frac{\hbar^2}{2}\sum_{A}^{N}\frac{1}{m_A}\nabla_A^2 - \frac{\hbar^2}{2}\sum_{i}^{n}\frac{1}{m_i}\nabla_i^2 - \frac{1}{4\pi\varepsilon_0}\sum_{A,i}^{N,n}\frac{e^2 Z_A}{\Delta r_{iA}} + \frac{1}{4\pi\varepsilon_0}\sum_{i<j}^{n}\frac{e^2}{\Delta r_{ij}} +$$

$$\frac{1}{4\pi\varepsilon_0}\sum_{A<B}^{N}\frac{Z_A Z_B}{\Delta R_{AB}} \tag{2.6}$$

The potential energy, V, component is the Coulomb repulsion between the pair of each charged entity such as treating each atomic nucleus as a single charged mass. It will be explained by using the equation (2.7). (Foresman 2016)

$$V = \frac{1}{4\pi\varepsilon_0}\sum_{A,i}^{N,n}\frac{Z_A e^2}{\Delta R_{Ai}} + \frac{1}{4\pi\varepsilon_0}\sum_{i<j}^{n}\frac{e^2}{\Delta r_{ij}} + \frac{1}{4\pi\varepsilon_0}\sum_{A<B}^{N}\frac{Z_A Z_B}{\Delta R_{AB}} \tag{2.7}$$

The equation for potential energy using Δr_{jk} is based on the distance between the two particles j and k, which goes for the particles at interest e_j and e_k (Foresman 2016). This can undergo mainly based on how they could work for the activity of electrons by obtaining the potential and kinetic energy using the valence-bond wavefunction for the electrons using the Hamiltonian in which we can see the electron and nuclear interaction and the electron-electron repulsion and also the nuclear-nuclear repulsion.

Thus, from the overall equation, we can eliminate a few terms that revolve around the nucleus due to Born-Oppenheimer's approximation by helping simplify the solutions to the Schrödinger equation. Born-Oppenheimer approximation states that the nucleus can be treated as stationary since the nucleus is heavier and slower than the electrons (Silbey 2005). This allows Hamiltonian to be written in terms of a model dependent parametrically on the nucleus and its coordinates (Strinati 2005). From this, we then go further to the Bon-Oppenheimer equation; we will need to remove the nuclear equation; the nuclear-nuclear repulsion from the equation is constant. This is what undergoes the Born-Oppenheimer approximation, which operates in the weak coupling of nuclear and electronic motion (Woolley 1976). This equation then translates how the wavefunction product of the Born-Oppenheimer wavefunction must be derived. In contrast, the electron-electron aversion this equation (2.8) from the Born-Oppenheimer is based on the electron.

$$H = -\frac{\hbar^2}{2}\sum_{i}\frac{1}{m_i}\nabla_i^2 - \frac{1}{4\pi\varepsilon_0}\sum_{i,A}\frac{Z_A e^2}{r_{iA}} + \frac{1}{4\pi\varepsilon_0}\sum_{i<j}\frac{e^2}{r_{ij}} \qquad (2.8)$$

In Equation 2.8, the r_{Ai} is the distance between an electron i and the nucleus A of the Charge Z_A, and r_{Ai} is a nuclear and electron attraction (Atkin 2014). While the r_{ik} is shown in the equation, electron-electron repulsion from electron i and electron k are mutual, as explained in

the Hamiltonian equation. The Schrödinger equation for being an equation to solve one of the simplest atoms led to the use of the Born-Oppenheimer approximation for the molecules based on their energy variations equation (2.6). However, as further it goes on, the born Oppenheimer becomes broader in calculating molecules. The eigenvalues become more complicated to solve over time by the different derivative values obtained mainly by the various coordinates and dimensions a molecule may have.

2.2 Methods

Methods in computational chemistry are used in a different approach to help calculate a computational solution for Schrödinger's equation. The method that is used is the *ab initio* methods which focuses on the approximate solution to the energies of Schrödinger's equation based only on the quantum mechanical law and theory that involves known physics constants and not experimental data. The *ab initio* method has been used for the molecular orbital in their dimensional approximations for the main interest by using derivatives for the electron distribution by calculating integrals for the atomic orbitals (Atesin 2014). *Ab initio* methods were also used for the application methods used for the wave function and the approximation in getting the exact energy function (McQuarrie 1997). They are all based on the laws of quantum mechanics by determining matrix elements and integrals for the function's geometrical degrees of freedom (Simons 2019).

This research has been on the *ab initio* calculation through all the experimental analyses throughout this thesis. The primary calculation techniques in this section and chapter focus on are Density Functional Theory (DFT) and Second-Order Møller- Plesset Perturbation Theory (MP2). My research used these methods for the computational calculation to explain their function in the Schrödinger equation's convergence. A technique that is also used based on the MP2 is the Hartree-Fock method (HF) because the unperturbed zeroth-order wavefunctions that are as input for MP2 are obtained from an HF calculation.

British physicist Douglas R. Hartree developed Hartree-Fock in 1927 and introduced the Hartree methods known as the self-consistent field (SCF) methods, and soviet Vladimir Fock 1930 worked with some part of getting an approximation following Hartree's work. In 1935 they

obtained a better approximation for the wavefunctions and the energies of a multi-electron chemical system (Hartree 1935). This collaboration was to obtain better approximations for the wave function and the energies of a multi-electron chemical system. Hartree-Fock is a good starting point for most cases, including the first step for a highly accurate approximation to solving the electronic Schrödinger's equation which arises because of the time-independent Schrödingers equation after the Born-Oppenheimer approximation model is being applied (Sherrill 2000). HF was designed to solve the time-independent Schrodinger equation electronic wave functions. HF focuses on considering the potential repulsive energy interactions from the electrons of interest and the average field generated that is distributed in the system by the rest of the electrons (Hanson 2021). HF involves treating the electronic wavefunction as a one-electron wavefunction combined into a single Slater determinant, as shown in equation 2.9.

$$\psi(r) = \frac{1}{\sqrt{n!}} \begin{pmatrix} \phi_1(r_1)\alpha(1) & \phi_1(r_1)\beta(1) \ldots & \phi_{n/2}(r_1)\alpha/\beta(1) \\ \phi_1(r_2)\alpha(2) & \phi_1(r_2)\beta(2) \ldots & \phi_{n/2}(r_2)\alpha/\beta(2) \\ \phi_1(r_n)\alpha(n) & \phi_1(r_n)\beta(n) & \phi_{n/2}(r_n)\alpha/\beta(n) \end{pmatrix} \qquad (2.9)$$

The best possible result of the one-electron wavefunction will have to yield to the lowest energy for a multi-electron system (Hanson 2021). Thus, the multi-electron problem system is then solved by considering a one-electron problem in which each spin of an electron is specified, and it will contain its own orbital. It will result in twice the number of orbitals accounting for the electrons and their corresponding spins. In equation 2.9, these symbols ϕ represents the orthonormal set of molecular orbitals from a range within 1 to $\frac{n}{2}$ taking into account the totality of the spatial orbitals (Foresman 2016). Then the variable n represents each electron with its specified spin that is being alternated as the label of the electron spin, n, and ranges from 1 to n.

In that case, the spin-up will be represented by α, and for spin-down, it will be represented by β. The slater determinant represents the antisymmetric electron wavefunction, which is used to derive the Fock operator from the Hartree-Fock equation 2.10.

$$\mathbb{F}\varphi_{(} = \epsilon_{(}\varphi_{(} \qquad (2.10)$$

From this equation, $\mathbb{H}$ is the Fock operator, which focuses on the giving energy and the HF orbital for the single electron. Equation 2.11 is what can best describe the derived Fock operator.

$$\mathbb{F} = KE + PE(nucleus - Electron) + \sum_{?@'}^{-} X2\mathbb{J}_{?} - K_{?}[\qquad (2.11)$$

In equation 2.11, the first two terms represent the kinetic energy of the electrons and the potential energy that regard the attractive force between the electron and the nucleus. The third term is the potential energy of a single electron interaction from the rest of the average electron fields. The $\mathbb{J}$operator is for the Coulumb operator that is dealing with the electron repulsive interaction, and K, the exchange operator, is relating to the change of orbital labels. Following the electronic wavefunction, it is applied as part of the Hamiltonian energy that can be calculated. Having the help of the variational method, the expected energy can be worked out to be lower even if it is greater than the actual ground energy. The energy of the Hartree-Fock can start by making an initial guess of the parameters of the spin orbitals from the Fock operator in the Hartree-Fock equation and solving for new sets of spin orbitals until it reaches self-consistency. The spin orbitals that yield the lowest electronic energy are the correct spin orbitals used to shape the lowest energy state of a molecule.

2.2.1 Density Functional Theory

Density Functional Theory (DFT) is a theory created by Hohenberg and Kohn in the 1960s, which is the method used in chemistry and physics to calculate the electronic structure of atoms, molecules, and solids (Hohnberg1964). DFT, as it rests on the Hohenberg-Kohn theorem, shows a 1- to -1 relationship between the density and the ground state properties of a system. A universal functional E(ρ) gives the ground state energy for the given density. The practical use of DFT is frequent; although not always, it relies on Kohn and Sham's work. They show that it is possible to obtain the ground state density of a system that includes correlated electrons by constructing a system of non-interacting electrons to prove they have the same density. The Kohn–Sham DFT would look similar to the Hartree–Fock. DFT is inexpensive since it uses less time from the computer and is one of the methods that always got agreeable experimental values of the other techniques used for the integrals of the atomic orbitals. In scientific-practical work, DFT is often used to calculate the molecular structure based on its function of including the effects of electron correlations of the molecular system of motion (Foresman 2016). DFT will determine the ground-state electronic energy by connecting functional designs, focusing on the electron probability density, ρ, a correspondence between the electron density of a system and energy (Atkins 2014). DFT was made to solve the Schrödinger equation by using the Hamiltonian as the energy expressed for the wavefunction of the ground state energy and exact density. In 1964, Dr. P. Hohenberg and Dr. W. Kohn determined that equation (2.12) calculated the probability of electron density for the electron molecule, N_e-, and demonstrated its ground-state energy.

$$E = E_T + E_V + E_J + E_{XC} \qquad (2.12)$$

This equation is based on another *ab initio* method Hartree-Fock (HF). In equation 2.12 $E_{T,}$ kinetic energy means the electrons' motion, the potential energy, E_V, of the nuclear-electron attraction, and E_J is the Coulomb of the electron-electron repulsion in the electron density (ρ)r (Shao 2014). In short, $E_{XC,}$ if separated into two E^X and E^C, is based on the average of HF methods of the electron-electron interactions. The broad E^X, pure exchange functionals are significant on the same spin of the strong electron repulsion force interaction with another electron (Foresman 2016). The exchange functionals energy goes as the functional exchange energy, the parameter γ is chosen to fit the exchange of energies, and Becke defines its value as 0.0042 Hartrees, then ρ(r) is the exchange of energies, and $\boldsymbol{\nabla}\rho$ is the gradient of the local functionals of the electron density. The minimal E^C is the correlation functionals of the extensive mixed-spin interactions of having a weak repulsion pulse of electrons of opposite spins. The correlation functionals equation goes as follows.

The correlation functionals variables go as this ε_c is the general expression of interpolation of mixed spin cases, r_s is the density parameter, and ζ is the relative spin polarization which contributes to α and β spins. The Density Functional Theory (DFT) used for this thesis was the B3LYP which stands for Becke gradient-corrected exchange functional, 3-parameter, Lee, Yang, and Parr gradient-corrected correlation functional (Lee 1988). This is a hybrid functional of the Hartree-Fock theory that Becke formulated in the formulation exchange, a mixture of Hartree-Fock and DFT. The hybrid density functional, B3LYP, is expressed in equation 2.13.

$$E_{\mathrm{AB}}^{\mathrm{i\ CDEF}} = (1 - a_{\cdot})E_{\mathrm{A}}^{\mathrm{DGH,}} + a_{\cdot}\,E_{\mathrm{A}}^{\mathrm{IJ}} + a_{\mathrm{A}}\Delta E_{\mathrm{A}}^{\mathrm{i\ KK}} + a_{\mathrm{B}}E_{\mathrm{B}}^{\mathrm{DEF}} + (1 - a_{\mathrm{B}})E_{\mathrm{B}}^{\mathrm{LM\ -}} \qquad (2.13)$$

The equation terms $E_{\mathrm{A}}^{\mathrm{DGH}}$ and $E_{\mathrm{B}}^{\mathrm{LM}}$ are correlated from the density functional by the approximation of the exchange and correlation functional spin density approximation. The exchange $E_{\mathrm{A}}^{\mathrm{IJ}}$ comes from the Hartree-Fock, for the correction gradient for the exchange functional is. The Perdew-Wang term $E_{\mathrm{B}}^{\mathrm{DEF}}$ is the gradient correction in the correlation functional. The Becke 3 parameter functional coefficients typical valuables that are placed in this method for the fitting of experimental data are $a_0 = 0.2$, $a_x = 0.72$, and $a_c = 0.81$ (Jensen 1999) (Foresman 2014) (Stephens 1994) (Daniels 2021).

2.2.2 Second-Order Møller- Plesset Perturbation Theory

Second-Order Møller-Plesset Perturbation Theory (MP2) is another *ab initio* method that effectively corrects the Hartree-Fock ground state energy, which describes the electron correlation effect (Del Ben 2012). MP2 approximates correlation energy molecules, mainly used for theory levels more than Hartree-Fock. MP2 is derived from the Rayleigh-Schrödinger perturbation theory, which includes a higher excitation in the Hartree-Fock approximation in the energy (Shao 2014). In this, the unperturbed Hamiltonian Operators is being divided and is written as

$$H = H_{.} + \lambda V \qquad (2.15)$$

The Hamiltonian correction consists of the lambda cap V hat, which is a perturbation applied in which λ is a dimensional parameter is very small, and cap V hat is a small perturbation expressed based on the power series on the perturbed wavefunction and energy (Foresman 2016) (Shao 2014). Then by adding correction by setting these two equations 2.16 and 2.17.

$$\psi = \psi^{(.)} + \lambda\psi^{(')} + \lambda^{"}\psi^{(")} + \lambda^{(C)}\psi^{(C)} + \cdots \qquad (2.16)$$

$$E = E^{(.)} + \lambda E^{(')} + \lambda^{(")} E^{(")} + \lambda^{(C)} E^{(C)} + \cdots \qquad (2.17)$$

The perturbed wavefunction and energy will be substituted back to Schrodinger's equation, as seen in equation 2.18.

$$XH_{.} + \lambda V[X\psi^{(.)} + \lambda\psi^{(')} + \lambda^{"}\psi^{(")} + \cdots [= (E^{(.)} + \lambda E^{(')} + \lambda^{"} E^{(")} + \cdots)(\psi^{(.)} + \lambda\psi^{(')} + \lambda^{"}\psi^{"} + \cdots) \qquad (2.18)$$

This expansion of these coefficients after setting them with the power of λ will lead them based on the representation of the highest orders of perturbation (Foresman 2016). So, these equations will be based on the energies multiplied based on the order of perturbation from the power of λ going from 0, 1, and 2, as seen in the equation set 2.19, 2.20, and 2.21.

First equation 2.19, the zeroth-order sine the H_0 is the sum of the Fock operators, so $E^{(0)}$ will be the sum of the orbital energies.

$$E^{(.)} = b\psi^{(.)}dH_{.} \mid \psi^{(.)}f = \sum_{(} \varepsilon_{(} \qquad (2.19)$$

Second, equation 2.20 of the first order correction is the sum of orbital energies counting twice electron-electron interaction and is the first order energy. Still, the second order is the first order.

$$E^{(')} = b\psi^{(.)}d\mathbb{V}a\psi^{(.)}f \qquad (2.20)$$

Third, equation 2.21, the second order energy correction, is where it three will be a linear combination of the substituted wavefunction and solve for the coefficient since the energy is close to the ground state, contributing to the perturbation.

$$E^{(")} = b\psi^{(.)}d\mathbb{V}a\psi^{(')}f \qquad (2.21)$$

The equations are based on the zeroth-order perturbation, where the correlation is on the sum of the energies of the spin orbitals (Shao 2014). The $E^{(0)}$ and $E^{(1)}$ are being summated by the representing $H_{.} + \lambda V$ of Hartree-Fock energy equivalent by the Hamiltonian operator. After determining $\psi^{(1),}$ then $E^{(2)}$ will be determined by having a correction. It will always be negative in the second perturbation of the energy of the spin-orbital, which is expressed in equation 2.22 (Foresman 2016).

$$E_{.}^{(")} = -\frac{'}{4} \sum_{YZ}^{W(X} \sum_{(?}^{UW} \frac{|Qabrijs|^{!}}{6_{)}\, T\, 6_{*}\, 0\, 6_{"}\, 0\, 6_{+}} \tag{2.22}$$

The MP2 correction arises by mixing the Hartree–Fock ground state determinant with the "double excitations" in which they differ from the ground state by taking the electrons from the occupied orbitals i and j and placing them to the previously occupied orbitals a and b. The numerator describes the Coulomb and exchange couplings between these orbitals arising from the electron correlation, and the denominator includes the orbital energy differences. The biggest corrections to the energy will arise when the coupling is large, and the difference in energy between the HF determinant and the doubly excited determinant is small.

2.3 Basis Sets

From section 2.2, we learned that HF and DFT are formulated without mentioning atomic orbitals. However, as a practical matter, we would need to express the molecular orbitals in a way that allows us to make an educated guess of what they should be by improving the guess. From what we know that the non-interacting electrons on a system with one nucleus will fill the hydrogen orbitals. Basis sets are an *ab initio* approximation for molecular orbitals in a molecule of mathematic representation (Foresman 1999). The molecular orbital of a linear combination of a one-electron system is expressed when represented in the electronic wave function. Basis sets express the linear combinations, calculate the different methods used based on their efficiency, and how they will correspond based on the methods used. Basis sets are implemented by different conditions by the scientist, like methods that will be used, molecular geometry, and the geometry of the molecule. This is where molecular optimization has some limitations in which role on how it will work. The individual molecular orbital, Φ_i, is defined by the following

$$\Phi_(= \sum_{[@} c_{[(\chi_[\qquad (2.21)$$

Equation 2.21 as of coefficient $c_{\mu i}$ is the molecular orbital expansion coefficient. Then χ_μ represents the basis functions from $\chi_1 \ldots \chi_N$, which will be normalized (Foresman 2016). So, the variational method will then be used to solve the best parameters in the molecular orbital expansion coefficients and basis functions. The parameters defined as the "best" will give the ones with the lowest ground state energy (Zielinski 2005).

The basis set 6-311++G was used for this research for the potential energy scan. Another basis set, aug-cc-pVTZ, was used for the geometry optimization.

The basis set 6-311++G is a Pople-style basis set (Krishnan 1980) for more atomic and valance atomic orbitals. It is used for calculations made to be used in the Gaussian software by Dr. John Pople and his research group (Ditchfield 1971). This basis set is considered "balanced" when there are diffusion and polarization functions and good quality results. However, this basis set is very expansive in terms of use for calculations based on the quality of measures that are being done. The 6-311++G is a triple split valence basis set. The core orbitals are a concentration of six Primitive Gaussian Type Orbitals (PGTO) and three functions having valence splits by representing PGTO. The first + indicates the diffusion in one set of s- and p- functions of heavy atoms, and the other + refers to a distribution of the s-functions of extra hydrogens in the molecule. The basis set of 6-311++G is a costly basis set since it uses much energy and takes time mostly since it's the highest basis set from Dr. Pople's basis set.

This basis set was mainly used for this thesis for the rotational scan, shown in chapter 4 in the data and the significance of its use. This handy basis set was of great use since it is for the derivation of the second and high row elements of calculations of the functions this basis set can calculate.

The aug-cc-pVTZ or the Augumented Correlation Consistent Polarized Split-Valence Triple Zeta is a basis set that Professor Dunning and partners proposed a new diffuse basis function for all atoms in every angular momentum on basis functions present in the atom (Papajak 2011). First, the aug- is denoted as augmented, which means that an extra diffuse basis function is added to each atom and angular momentum such that the basis set is augmented fully. Using nonafluoro-tert-butyl alcohol as an example, you will have the addition of diffuse s, p, d, and f subshells on the carbon atoms. This will help to accurately represent the atomic orbitals that have a far distance from the Carbon atom. Seconds, the cc- it stands as correlation consistent

and is a type of extended basis that adds up shells of functions to the atomic functions of Hartree-Fock (Hill 2010). Third, the “p” it stands for polarized and considers the inclusion of polarization functions that contain an additional node, and it allows the orbitals to be more asymmetric towards the atomic nucleus. Moreover, this will create the ending effect of expanding the basis set and the basis set to obtain accurate calculations by allowing additional flexibility. Fourth, the “VTZ” ending is known as valence triple zeta, and it utilizes 3 slater-type orbitals (STOs) to represent a single atomic orbital. This includes the splits valence and linearly combining two orbitals from the same type but with different effective charges. These terms increase of quality by each type of each one of the basic functions it will add a new kind of high order polarization function (Jensen 1999). For example, aug-cc-pVXZ having a part of the angular moment, can play subshells from primitive functions and contracted functions which is a basic set that recovers the correlation energy of valence electrons. However, the basis sets are interested in recovering core-core and core-valence electron correlation functions; thus, all the acronyms such as aug-cc-pVTZ have considerable intimate parts. This aug-cc-pVTZ is a huge basis set that can introduce the possibility of having a variety of different atomic orbitals that could be chosen of the molecular orbitals.

This basis set was used for the fundamental research of the thesis using for the calculations for the entire simulated experiment. This was used with both methods, MP2 and DFT. The rest of the data will be shown what it got of numbers, and being the critical basis set of the experiment, will be able to offer the information regarding this basis set.

2.4 Hardware

There are many other high-performance computing centers worldwide for the same type of interest in universities to get various data for the types of analysis they are placed on and what they are focusing on. In regard to the supercomputer, there is a question on how it became famous for research and development in the science and engineering fields in the 1950s (Pritchard 2001). Seymour Cray's company created the first supercomputer, Cray-1; it was first known in the late 1970s to perform a large-scale scientific application for the physical phenomena of 240 million calculations per second (Jensen 1987). This supercomputer then started being sold to the government and the universities. This became popular for research in many fields of science (Jensen 1987). Including the innovation in making their supercomputer for it to be used in their lot of research by increasing their calculations minutes and time range of the stimulations. Therefore, today we have 165 supercomputers nationwide in the United States for research development of any study of physics, chemical, biological, pharmaceutical, and environmental (Service 2016). These supercomputers have helped understand the stimulations and the calculations on the atom or compound being analyzed in the research (Jensen 1999). The supercomputer works in the molecule's vibrational frequencies and the interatomic motion within the molecule (Foresman 2016).

Figure 2. 1:Seymour Cray with his Cray-1 Supercomputer

Computer History Museum. Supercomputer designer Seymour Cray in front of his Cray-1 computer. (n.d.). Retrieved May 19, 2022, from https://www.computerhistory.org/revolution/supercomputers/10/7/3

The computer center used for our calculations is the Texas Advanced Computer Center (TACC). It's at the University of Texas at Austin. This is where science and engineering send their analysis and can send their respected data to be calculated into the computing center. For example, TACC has been used as a resource for covid-19 to underline its effects within the virus itself, making this an interest in scientists and medical investigators to understand how to simulate its atoms by 2020. TACC has been the aid for the computational work for the experimental work that has been used for most of our studies in having a set of views on how the molecule we are studying works. TACC has also advanced its investigation by looking based on the earthquake and tsunamis in the environment's radiation by using their Lonestar4.

2.5 Software

As a primary focus of the softwares used in this project were Gaussian, and Pgopher for the molecule we have been analyzing through our years of work. Gaussian was the program used to get the geometric structure of our molecule. Pgopher is a program used to simulate our calculated results from our molecule that had been calculated through TACC. These software have been a great aid in looking at the experimental and the simulated work based on what is done with the alcohol we are researching and to be able to understand its stimulation. Also, in getting our structure geometric structure in order to get its calculations for the further in getting the structure correctly when wanting to have the correct data to get calculations.

The primary software used in this research in this thesis has been Gaussian and Pgopher, which will be explained more in this chapter.

2.5.1 Gaussian

At the University of Cambridge in England, Dr. John A Pople and his research group created Gaussian, an ab initio quantum chemistry method (Hehre 1970). He developed this computational method by using the basis sets by modeling the wave functions of the orbitals. By creating this software, it was easier to be used for the plans and basis sets that were used since it was costly to use these computational methods to be solved. Thus, this system pioneered having a more accessible way of forming the molecule or atom to get scientists and students to work on getting a faster computational method than sending their job to the supercomputer. Gaussian software was created in 1970 in which. Pople was a pioneer in developing this computational method for molecular structures. This software has been called an *ab initio* quantum chemistry method since most of his research was based on the electronic structure theory. However,

Gaussian was not the only program that conducted molecular optimization in time since there were other programs used for investigation in this type of quantum chemistry methods in electronic structure. Gaussian 70 was the program that was preferable to use for molecular observation by its efficiency and how easy it is used. Professor Pople was not only one of the pioneering scientists in the program Gaussian but of the development of Perturbation Theory, Couple-Cluster method, modern calculations of Hartree-Fock, Self-Consistent Field (SFC), and basis sets that are used when analysis today.

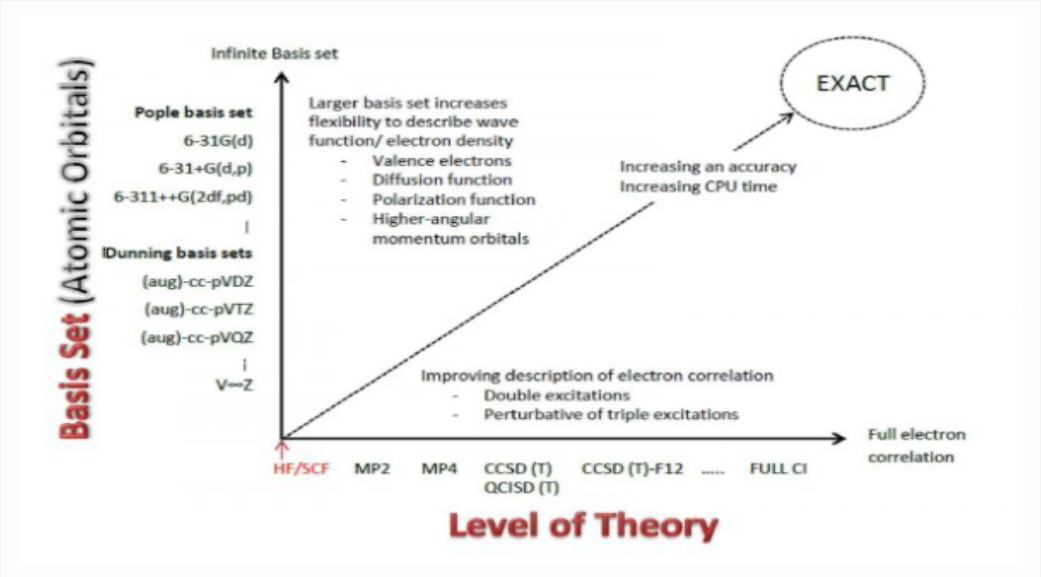

Figure 2. 2: Pople Diagram of Basis set for Gaussians software for atomic orbitals

Gaussian software has kept up with modern computational chemistry developments by updating and optimizing its programs. The most current Gaussian software used for this time in the thesis is Gaussian 16. This software is run by a supercomputer such as TACC, in which the molecule is being simulated in its optimization of the structure of our molecule is being analyzed. Chemical quantum calculations are doing this work. The molecule is being

theoretically observed and optimized by the system by combining the Gaussian software and supercomputer abilities of TACC.

2.5.2 Pgopher

Pgopher is software that has been used for microwave spectrum stimulations such as vibrational, electronic, and rotational spectra of a molecule (Western 2017). As all the calculations are obtained, the optimized molecular structure from the ab initio calculation Gaussian 16 will give rotational values calculated. These rotational values of the molecule will provide us with the molecule's information of its characters so it can be simulated in a microwave spectrum. Rotational Values that are being used are the rotational constants (that are known as A, B, C), dipole moments (a, b, c), and the centrifugal distortion constants (DJ, DJK, DK). This can be used for any molecule simulated in Pgopher based on their symmetry can have poor fit based on the calculated values based on these parameters.

The rotational parameters A, B, C will be discussed in more detail in Chapter 3 and will be explained on why these are important to know. As the same will be for the dipole moment and the centrifugal distortion constants and why we need to know them and their importance in the stimulations when doing Pgopher.

CHAPTER III

ROTATIONAL SPECTROSCOPY

3.1 Introduction of Rotational Spectroscopy

At the start of this chapter, we must start with a question about what is spectroscopy, why is it important, and what does it study? First, spectroscopy is the study of the absorption and emission of light and of scattering by electromagnetic radiation by atoms and molecules (Hanson 2022). We have emission and absorption spectroscopy they have different frequency of light for specific types of motion and why? Thus, emission spectroscopy is where the electromagnetic radiation arises by a transition that a molecule is undergoing from the detection of high energy state to a low energy state and its frequency is being analyzed (Atkins 2018). Absorption spectroscopy is the net absorption radiation that passes through a sample that is being monitored from a range of frequencies and stimulate the emission radiation. They both give the same information in regards of the energy levels separation for vibrational, electronic, and rotational. From the information we now understand of spectroscopy we can know focus on the different methods in spectroscopy.

Rotational Spectroscopy or Microwave Spectroscopy is a technique that helps identify the values that precisely define the structure and identity of molecules. The molecule's characteristics, such as bond lengths, angles, number of conformers, and dissociation energy, could be obtained with high accuracy (Atkins 2017). There are different types of spectroscopies, such as Nuclear

Magnetic Resonance (NMR), Fourier Transform InfraRed (FTIR), and Gas chromatography-mass spectrometry (GCMS), and there are also other overlooked spectroscopies that are less common. As explained, microwave spectroscopy is an analytical method that is used for the detection of the rotational transition of a molecule. These experiments are done in a chamber that has been kept in a high vacuum to minimize interference of impurities on molecules. The molecule is placed on a gas carried that will enter the chamber of a pressure background through a pulsing nozzle in which molecule undergo supersonic expansion through this process. While in the chamber, the molecules are in the energy ground-state. The incoming microwave radiation will move them into the excited state. All molecules like to be in the lowest energy state. Once the radiation stops, they will return to the ground state and emit radiation. The radiation is associated with the rotational energy levels. These transitions are detected in time domain and Fourier transformed into frequency domain. Microwave spectroscopy covers from the wavelength of 10^3 μm to 10^6 μm or approximately 3,000 MHz to 3,000 GHz (Stedwell 2013). This is shown in Figure 3.1.

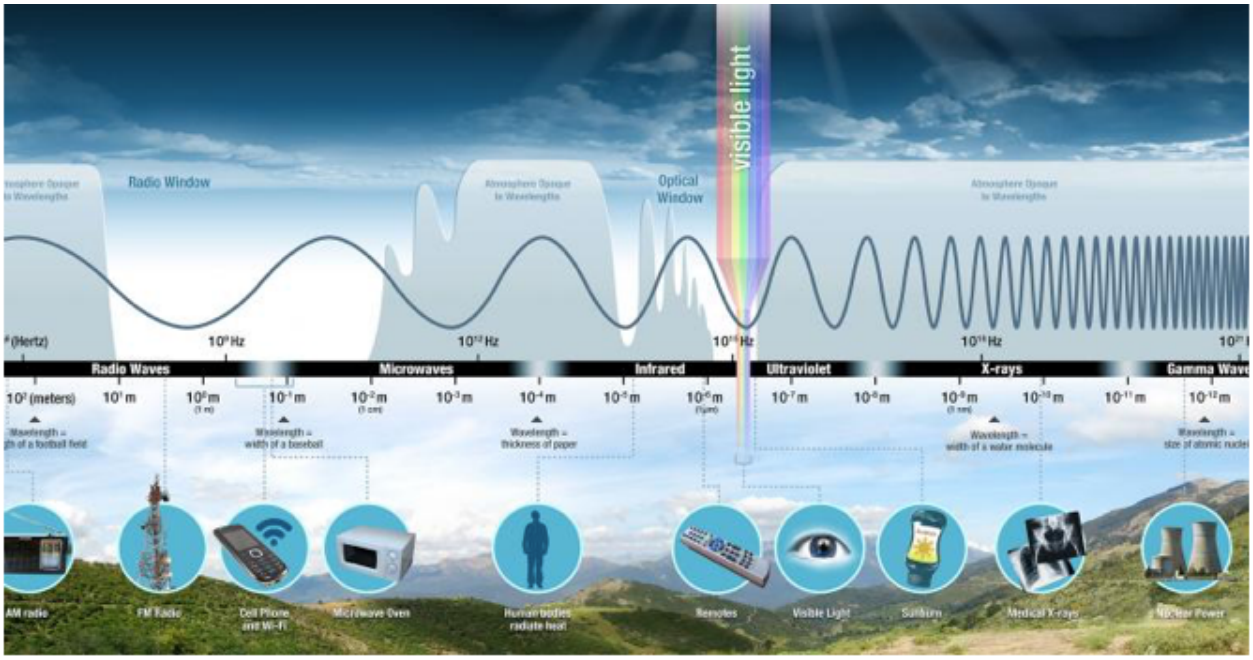

Figure 3. 1: Electromagnetic Spectrum

National Aeronautics and Space Administration, Science Mission Directorate. (2010). Introduction to the Electromagnetic Spectrum. Retrieved *June 15, 2022*, from NASA Science website: http://science.nasa.gov/ems/01_intro

During the 1940s the measurement of microwave frequency had been done by Claud Edwin Cleeton and Neal Hooker Williams for the microwave radiation of Ammonia (NH_3) (Gordy 1983). This is what brought the start of microwave spectroscopy advancing in the studies of scanning molecules creating new branches for research. As the technology advance to computers, microwave spectroscopy started to become efficient and less tedious when conducting research. The Fourier transform microwave spectroscopy was invented in early 1980, which allows data is being collected for the time domain and converted into the domain for frequency for simple interpretation of data (Alonso 2021). This is where the microwave

spectroscopy and Fourier transform had revolutionized with the computer development. Then by 2006 the first Chirped-Pulse microwave spectrometer was built and making a breakthrough in microwave spectroscopy.

The main reason for focusing on this part of spectroscopy is because the spectrometer used for this thesis was the Chirped-Pulse Fourier microwave spectrometer. This will be explained in greater detail in this chapter to understand the use of this spectrometer and its importance and what was analyzed experimentally in chapter 4.

3.2 Principles of Rotational Spectroscopy

Rotational Spectroscopy uses microwave radiation to measure the energies of rotational transitions of gas-phase molecules. The rigid rotor model assumes the distance between particles that will not distort under rotational stress (Fayed 2014). The molecular rotation is based on the molecules being defined by their mass based on the moment of inertia. Moment of inertia is which measures the object's resistance to the changes in the rate of its rotation; this equation is 3.1.

$$I = \sum_{(} m_{(} r_{(}^{"} \qquad (3.1)$$

From the equation 3.1, the I is the moments of inertia of a molecule of an axis that is passing through the center of the mass, m_i it is the mass of the atom i that is treated as a point and the r_i is the perpendicular distance from the axis rotation (Atkins 2018). Which does moment of inertia go through a torque of the axis I_a, I_b, and I_c in next section 3.3 we will see how the moment of inertia provides on how the axis of a molecule based on the symmetry. The molecules within each category can have different characteristics, including symmetry operations and dipoles. Thus, rigid rotors can be classified into four types of rotors. It is essential to know their categories based on their geometric structure and the inertia around the three orthogonal rotational axes shown in Table 3.1.

Table 3. 1:The four different types of Geometric structures of rigid rotors

Linear & Diatomic molecules		$I_a = I_b$, $I_c = 0$
Spherical tops		$I_a = I_b = I_c$
Symmetric tops	Oblate	$I_c > I_a = I_b$
	Prolate	$I_c = I_b > I_a$
Asymmetric Tops		$I_a \neq I_b \neq I_c$

As explained in Table 3.1, these geometries are characterized based on the moment of inertia designating the internal axis systems of rotation from three mutually perpendicular axes such as a, b, and c. These a, b, c- principal axis systems rotate together within the molecule and are then converted as the principal moments of inertia from the geometric structures known as I_x, I_y, and I_z or as I_a, I_b, and I_c, with the axes chosen as $I_V \geq I_Z \geq I_Y$. These chosen axes I_c is the largest moment of inertia, and I_a is the smallest since a-, b-, and c- are chosen to ensure the inequality (Bernath 2020). This will be explained in the next section were we will see how the body-center principal axis and moment of inertia are obtained.

For example, rigid linear or diatomic molecules rotate in free space (Lopez 1995). So, when looking at the diatomic molecule you will have a simple geometric structure with its atoms passing through one main axis. Since there is only one fixed axis to look at only one rotational constant, B, since it is used to describe the rotatory movement of the molecule. Thus, as the

molecule gets more complex in regards of the geometry and symmetry it utilizes all 3-dimmensional axis, and has two additional constants, A and C, which helps on describing the rotatory motion of the molecule. This can be noted that the figures it is not in a typical cartesian coordinate system. they are in the principal axis system. It is chosen to describe the rotations of the molecules more conveniently.

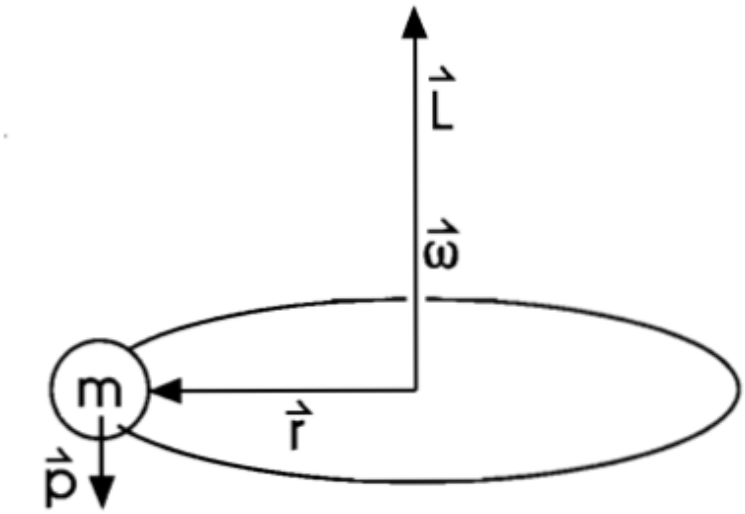

Figure 3. 2: Circular motion

Bernath, P. (1995). Spectra of Atoms and Molecules (4th ed.). Oxford University Press.

In Figure 3.2, we can see a particle is moving in a fixed axis and it is undergoing through circular motion. The mass is moving at a constant speed $\vec{p}$ around a circular path of a radius from (x,y) plane which r is the origin of the Cartesian coordinate system. As the motion period is *T* and the frequency of motion is *f=1/T* then with the Newton Law of motion, F=ma is where the direction is going towards the in which the center of the mass. The particle is rotating with an angular velocity ω is from the center of the mass as it connects from the circular motion towards the angular moments in where the movement from the particle.

Since we are focusing on the rotational system of a molecule and what we know regarding a linear system must be changed in terms of the rotational systems. The equation found in Table 3.2 are important to have when going over the motion when focusing on a linear motion system to an angular motion system. This is very important in being familiarized with the angular motion system, since in this thesis this discussion will be in terms of angular motion.

Table 3. 2: The Angular and linear motion relation

Linear motion		Angular Motion
Distance, x	*Position*	Angle, θ
Velocity, $v = \dot{x} = \frac{!"}{!\#}$	*Velocity*	Angular Velocity, $\omega = \dot{\theta} = \frac{!\$}{!\#}$
Acceleration, $a = \ddot{x} = \frac{!\,!\,"}{!\,\#^{!}}$	*Acceleration*	Angular acceleration, $\alpha = \ddot{\theta} = \frac{!\,!\,\$}{!\,\#^{!}}$
Mass, m	*Mass*	Moment of inertia, $I = mr^{\%}$
Linear Momentum, $p = mv$	*Momentum*	Angular momentum, $L = I\omega$
Kinetic energy, $E_{\&} = \frac{'}{\%}mv^{\%} = \frac{(!}{\%)}$	*Kinetic Energy*	$E_{\&} = \frac{1}{2}I\omega^{\%} = \frac{L^{\%}}{2I}$

Now, we can take a moment to discuss some of the rotors, spherical top molecules. These molecules cannot be absorbed through electromagnetic radiation since they do not have a dipole moment that can be permanent (McQuarrie 1997), which is part of why they are not seen in a

microwave spectrometer. As seen in Table 3.1 the spherical top moment of inertia is equal on each axis $I_Y = I_Z = I_V$.

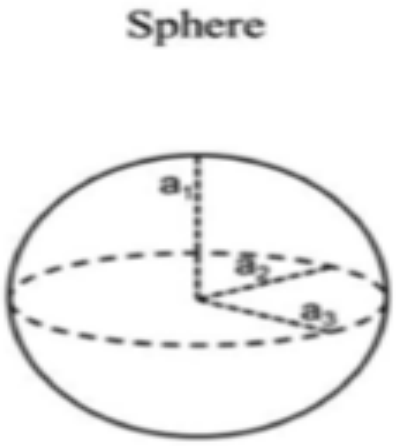

Figure 3. 3: Spherical molecule rotor

Kot, D., Kissinger, G., Schubert, M. A., & Sattler, A. (2017). Current stage of the investigation of the composition of oxygen precipitates in Czochralski silicon wafers. *ECS Journal of Solid State Science and Technology*, *6*(4), 17–24. https://doi.org/10.1149/2.0081704jss

Some examples of spherical top molecules are sulfuric hexafluoride (SF_6), methane (CH_4), and Silane (SiH_4). Since these molecules cannot be studied in microwave spectroscopy, it does not mean they can be studied in Raman Spectroscopy. The lack of dipole moment causes a problem for them being studied in rotational spectroscopy.

The next rotor will be Symmetric top molecules with two equal moments of inertia and one with a different moment of inertia by the rotational axis (Atkins 2018). We will see two types of molecules oblate and prolate, as shown in Figure 3.4.

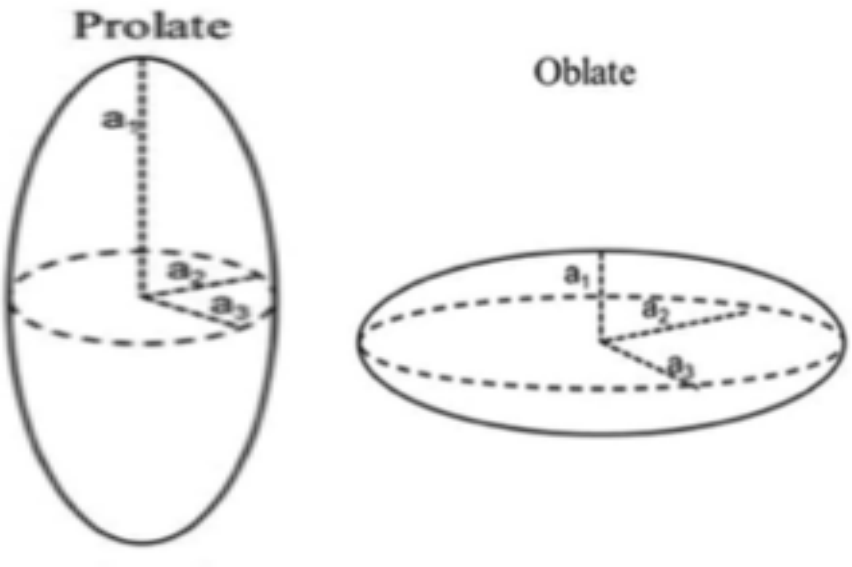

Figure 3. 4:Oblate and Prolate molecule rotors

Kot, D., Kissinger, G., Schubert, M. A., & Sattler, A. (2017). Current stage of the investigation of the composition of oxygen precipitates in Czochralski silicon wafers. *ECS Journal of Solid State Science and Technology*, *6*(4), 17–24. https://doi.org/10.1149/2.0081704jss

Figure 3.4, the moment of inertia they are dependents of the I_c axis. The moment of inertia is defined by the body's resistance to other forces because greater inertia means there will be a greater resistance in the axis. Such as, oblate top figure its I_c axis it resistant to the motion and prolate top figure is going to resist less to the motion and this could be regarded towards their shapes prolate look like a vertically placed cigar and oblate looks like a horizontally flipped egg.

Symmetric top will have rotational constants for the energy levels, also additional quantum numbers for the rotational energy level description (Bernath 2020). The energy levels correspond to the J value but when we include the asymmetry parameter κ this corresponds that

we have *2J+1* distinctive energy levels, but each have *2J+1 M*-fold degeneracy. This is where it defined (A-B) > 0 and (C-B) < 0 as the given values *J* the K_a will increase in energy as the K_a will increase for the prolate top. As the same for the K_c levels of energy be decreasing as the K_c increased for the prolate. The levels are labeled by J_{KaKc} in which J is a great quantum number the K_a and K_c are numbers used for the symmetric top limits and asymmetric top and their sum is from *J* or *J+1*. For the asymmetric parameter κ runts from the *K= -1* prolate top to *K=+1* oblate top. When K=0 it means is a degenerate (*2J+1*) fold the molecule follows the asymmetric top, and the $K \neq 0$ it has a 2(2J+1) fold degenerate, however the symmetric top selection rule will add $\Delta J = \pm 1, \Delta M_{\backslash} = 0, \Delta K = 0$.

Finally, in asymmetric top molecules, all three moments of inertia are not equal Table 3.1. Schrödinger's equation solution can be attained using the symmetric top basis set. Ray's asymmetry parameter can be used to describe the level of asymmetry on the deviation from prolate/oblate molecules shown in equation 3.16 (Bernath 2020).

$$k = \frac{"; 0, 0B}{, 0B} \qquad (3.16)$$

The asymmetric top selection rules are complex and dependent on the 3 dipole moments μ_a, μ_b, and μ_c, in which the rules will consist of $\Delta J = 0 \pm 1$, and $\Delta M_{\backslash} = 0, \pm 1$. Since these separations happen in different ways only for K_a and K_c. From following the a-type transition $\mu_Y \neq 0$ and $\mu_Z = \mu_V = 0$, $K_Y = 0, (\pm 2, \pm 4 \ldots)$ and $K_V = \pm 1, (\pm 3, \pm 5 \ldots)$ the values parenthesized from K_a and K_c meaning the transitions are weaker meaning that they will not likely happen. In the b-type transition, $\mu_Z \neq 0$, and $K_Y = K_V = \pm 1, (\pm 3, \pm 5 \ldots)$. Then for the c-type transition, $\mu_V \neq 0$ so $K_Y = \pm 1, (\pm 3, \pm 5 \ldots)$ and $K_V = 0, (\pm 2, \pm 4 \ldots.)$. These are the selection rule cases that can be seen in Figure 3.5.

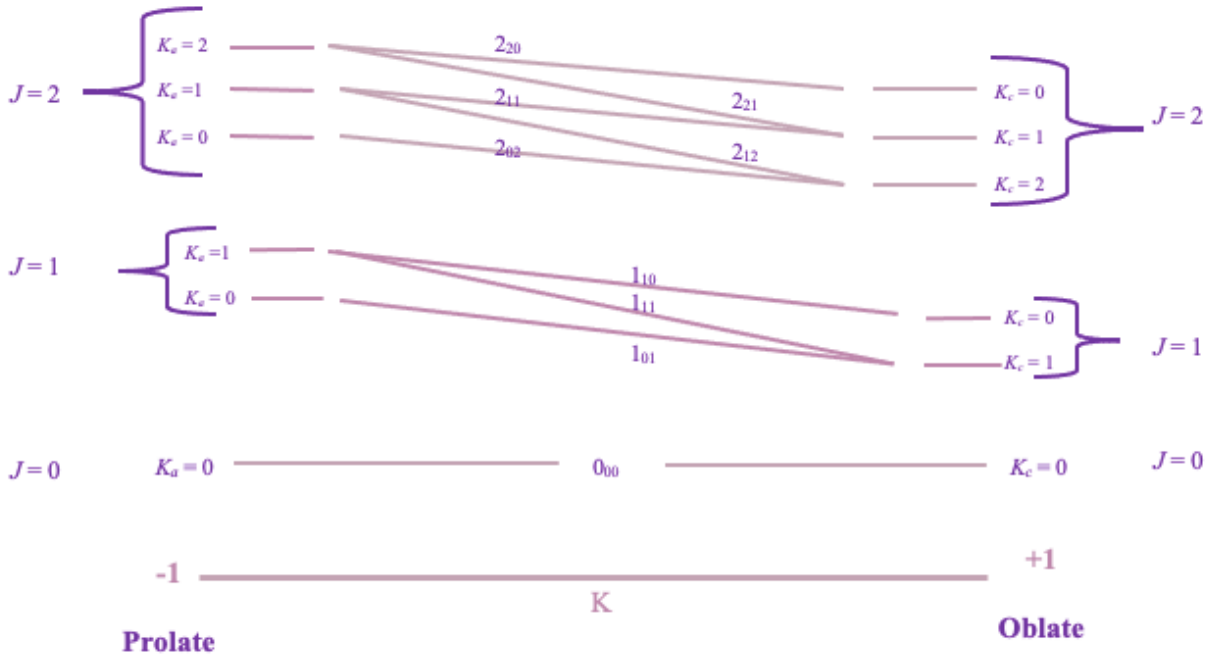

Figure 3. 5: Asymmetric top selection rules

3.3 Rigid Rotor

The main reason for talking about these rigid rotors in my thesis is because my molecule is an asymmetric top molecule. Nonafluoro-tert-butyl alcohol since we will go more in-depth in chapter 4 to dive more into understanding this molecule.

An example that will be used of the rigid rotor would be the diatomic molecule's distance since it is the one that has been used in other books on physical chemistry shown in Figure 3.6.

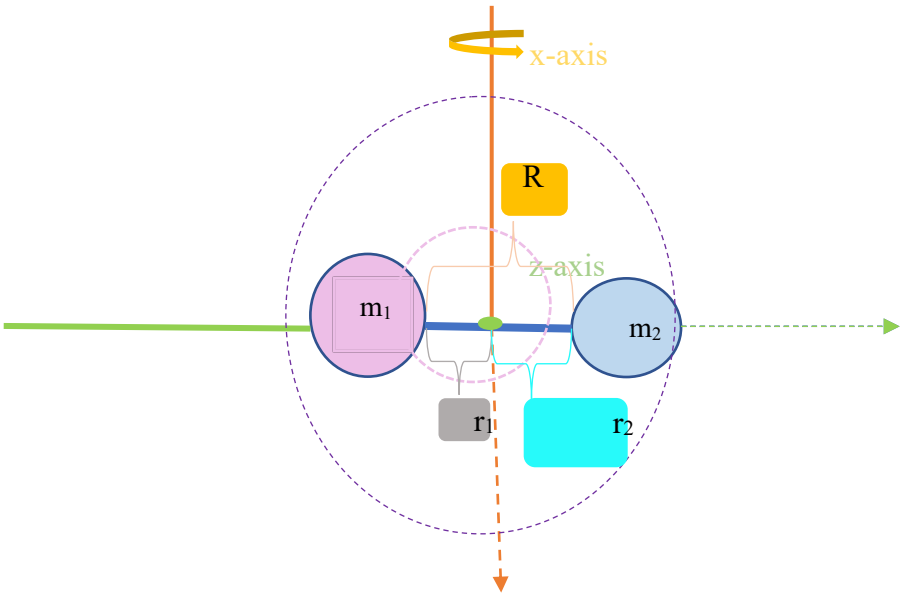

Figure 3. 6: Rigid Rotor model

This model is known as rigid rotors, consisting of two-point masses m_1 and m_2 with a fixed distance of r_1 and r_2 from the center mass. This distance between them has a stiff and rigid bond between two different atoms. Their unequal masses are symbolized in the light purple and blue circles. Also, the masses have unequal distances through the axis of rotation as it is passing within the center of mass that is symbolized in the small light green circle.

The model of the rigid rotor of the diatomic molecule goes based on how this molecular model is based on its energy. The diatomic molecule consists of two atoms that are bonded together. Anyhow, it's not a simple atom since the molecule needs to have dipole moments for rotational spectroscopy. If the molecule is without the dipole moments, it will not work in the observation of the rotational spectroscopy. For any categories in Table 3.1 case would be a fact. For example, molecules like H_2, N_2, and O_2 have no dipole moments, so they are not observed in rotational spectroscopy. However, the rotational spectra can be observed for HF, CO, and HCl since they have dipole moments. Since the rigid rotor represents the rotation motion of the molecule and it does not consider the stretching of the molecule as it rotates. However, a non-rigid rotor does consider the stretching and therefore labels it as centrifugal distortion. This will be covered more later in this chapter.

As explained in Chapter 2, quantum mechanics is a set of laws and concepts describing particle levels' motion at the atomic and subatomic. Applying the time-independent Schrödinger's equation helps explain a system's energy and information in detail for quantum mechanics.

The classical mechanics for the rigid rotor's general expression is

$$E_2 = \frac{'}{''} I\omega^{''} \qquad (3.2)$$

where ω is the angular velocity of the axis and I_k corresponds to the moment of inertia in which the rotational properties of any molecule could be expressed based on its three mutual perpendicular axes. This equation is composed of the kinetic energy on the Hamiltonian operator since the molecule is constantly in motion. This is also by excluding the potential energy in the equation because there is no resistance to the rotation (Castellan 1983). Equation 3.1 of the

moment of inertia considers the atom's mass and the perpendicular distance from the rotary axis. The rigid rotor would overall expression considering the x- and y- coordinates motion as shown in the equation (3.3) below.

$$E_2 = \frac{'}{"} I_{\&}\omega_{\&}^{"} + \frac{'}{"} I_{*}\,\omega_{*}^{"} \qquad (3.3)$$

Now talking of coordinates, we can now focus on what Cartesian coordinate and principal axis coordinates. Cartesian coordinates are what one in specifying the location of a point in the plane or a three-dimensional space like the *x*-axis*, y*-axis*, and* z-axis which are real numbers. The principal axis system is when the coordinate system is diagonal within the inertia tensor by having three perpendicular principal axes (Cline 2020). Principal axis systems are fixed to the shape of the rigid body and they are constant to the orientation from the body fixed coordinate system that are used to evaluate the inertia tensor. The system results of $I_{\&} = I_{*}$ and $I_{+} = 0$ as this expression is being described as having $x = a$, $y = b$, and $z = c$ (Atesin 2014). As they are written as $I_{\mathrm{Y}} = I_{\mathrm{Z}}$ and $I_{\mathrm{V}} = 0$, which overall will resemble table 1since the rotational constants are inversely proportional, meaning a, b, and c have the same relationship as I_{Y}, I_{Z}, and I_{V}.

The moment of inertia, for the rigid rotor, for I_{Y} and I_{Z} it will be equivalent to

$$I = \mu R^{"} \qquad (3.4)$$

In which μ is

$$\mu = \frac{\#_{,}\#_{!}}{\#_{,}\mathrm{T}\#_{!}} \qquad (3.5)$$

and

$$R = r_1 + r_2 \tag{3.6}$$

The reason is that the equation corresponds basely to a one-body problem and not a two-body system (Lopez 1995). The system considers the center of mass and the center of axis rotation.

The classical mechanics from equation 3.2, the rigid rotor from the kinetic energy can be adjusted as

$$E_2 = \frac{L^2}{2I} \tag{3.7}$$

rewriting $E_2 = \frac{1}{2} I\omega^2$ to $E_2 = \frac{1}{2}\frac{I^2\omega^2}{I}$ and then by switching L for $I\omega$. The equation of the moment of inertia directly will be in terms of angular momentum, L. The angular momentum of equation 3.7 will be replaced with the $\hat{L}$ symbol, which will indicate the quantum mechanics of the total angular momentum. The equation of classical mechanics of equation 3.8 will interpret as Hamiltonian quantum mechanics.

$$\hat{H} = \frac{\hat{L}^2}{2I} \tag{3.8}$$

After the Hamiltonian solution is added to the time-independent Schrödinger's equation, it will help solve the eigenfunction of the rigid rotor and the spherical harmonics in which

$$\hat{L}^2 \psi_{J,M} = \hbar^2 J(J+1)\psi_{J,M} \tag{3.9}$$

so, the eigenvalue will be solved to become

$$E = \frac{\hbar^2}{2I} J(J+1) \tag{3.10}$$

Instantly, by getting to this place now, we can properly bring in the rotational constant, B, which would be equal into

$$B = \frac{\hbar^{!}}{"]} \qquad (3.11)$$

Then equation 3.10 will be then turned to

$$E = BJ(J+1) \qquad (3.12)$$

The rules for diatomic/liner molecules of selection, $\Delta J = \pm 1$ (Bosanac 2001). An example of a selection rule that can be interpreted for the energy diagram for the rigid rotor will be denoted in Figure 3.7.

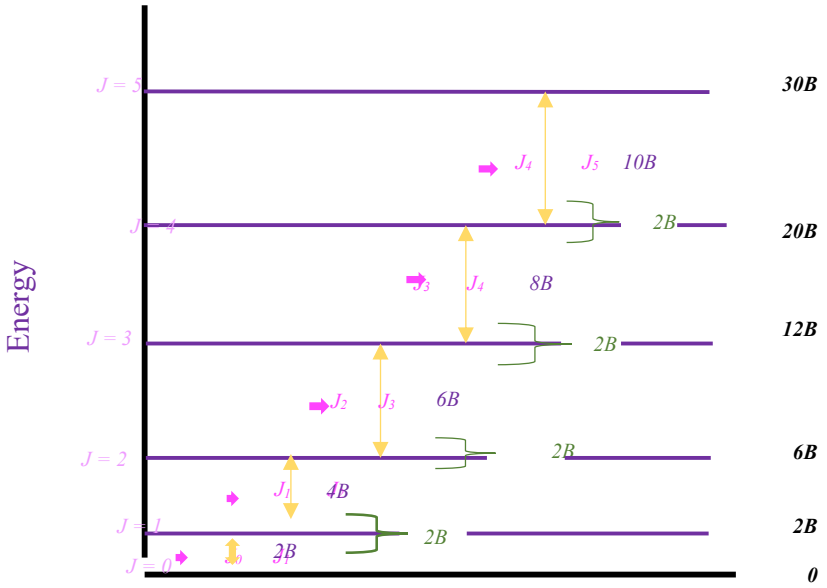

Figure 3. 7: Diatomic/ Linear Molecule selection rule

The J values (J = 0,1,2…) are incorporated into having different multiples spacing of the 2B energy regarding the rotational transitions E_J and E_{J+1}. The difference in energy levels can be expressed in equation 3.13

$$\Delta E = E_{\backslash T'} - E_{\backslash} = \frac{a^{!}}{45^{!}b}(J+1) \qquad (3.13)$$

The equation then can be based on the rotational constant B for equation 3.14

$$\Delta E = 2B(J+1) \qquad (3.14)$$

In which equation 3.15

$$B = \frac{a^{!}}{K5^{!}]} \qquad (3.15)$$

is in the units of frequency Hertz, Hz (Struve 1989), and the rotational transition have different separation by the 2B space. The spectra line in the rotational spectrum is shown in the energy diagram and multiplied by 2B, spreading them to represent their rotational transition. Based on this rotational spectrum, there will be lines spaced out by 2B when the rigid body is designated for the molecule.

3.4 Centrifugal Distortion Constant

As we have discussed in section 3.3, the rigid rotor about having a fixed distance while it is in its rotation. The rigid rotor is a theoretical model in which we restrict the distance between molecules to a rotation's particular value. In truth, the distance is not fixed as the molecules go through rotational transitions and the J value increases, the fluctuation of the bond distance, r. Bonds can compress or stretch a bit and increase the intensity as the energy of transitions increases. This is what centrifugal distortional means. The centrifugal distortion constant is known as the parameter D_J since we consider the stretching motion of the molecule in the middle of a natural rotation. In which a molecule rotates, it is not stiff as the rigid rotor explained theoretically. Thus, a molecule that rotates on a 3-D space can have bond stretching when it is rotating faster. A picture that can portray the stretching motion of the molecule as it rotates will be figure 3.8. It conveys the related mass on a spring and from the physics equation Hooke's law or the harmonic oscillator in studying the vibrational behavior of the molecules in between atoms.

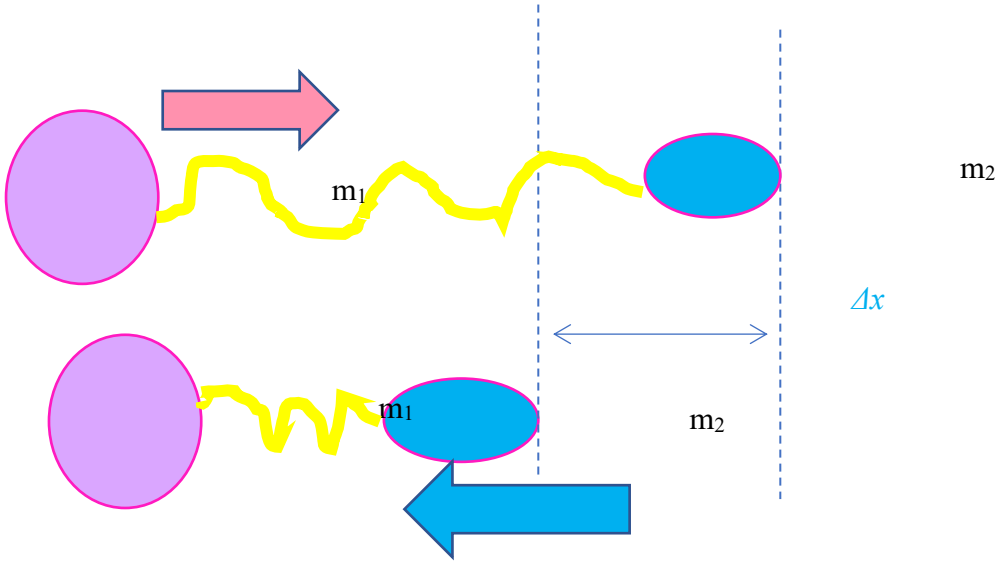

Figure 3. 8: Centrifugal distortion constant describing the stretching motion

From Schrödinger's equation, the Hamiltonian takes into consideration the centrifugal distortion constant, as seen in equation 3.17

$$\hat{H}_{CD} = -D_J \hat{J}^4 \qquad (3.17)$$

This is the correction added to the original Hamiltonian of the rigid rotor in which the constant D_J is

$$D_J = \frac{4B_e^3}{\omega_e^2} \qquad (3.18)$$

In equation 3.18, B_e stands for rotational constant, and w_e are connected to the vibrational frequency (Hollas 2002). Then equation 3.19 shows the eventuating energy from a rigid rotor alone after the centrifugal distortion correction had been added from a rigid rotor case.

$$E_J = BJ(J+1) - D_J(J(J+1))^2 = \Big(B - D_J J(J+1)\Big) J(J+1) \qquad (3.19)$$

Talking of the transition spacing of the spectrum in a more concrete way the correction of the centrifugal distortion constant is expressed in equation 3.20.

$$E_{\backslash T'} - E_{\backslash} = B[(J+1)(J+2) - J(J+1)] - D[(J+1)^{"}(J+2)^{"}]$$

$$= 2B(J+1) - 4D(J+1)^{C} \qquad (3.20)$$

The molecule as rotates fast, and with the J values increasing, the centrifugal distortion correction can be negligible on having a considerable effect on the spectrum. Then this correction of the centrifugal distortion constant will make the spectra lines be closed together by the expansion in the bond lengths, and the moment of inertia will result in a lower rotational constant value. The centrifugal distortion constant effect of a rigid to a non-rigid body from a rotational spectrum will be shown in Figure 3.9.

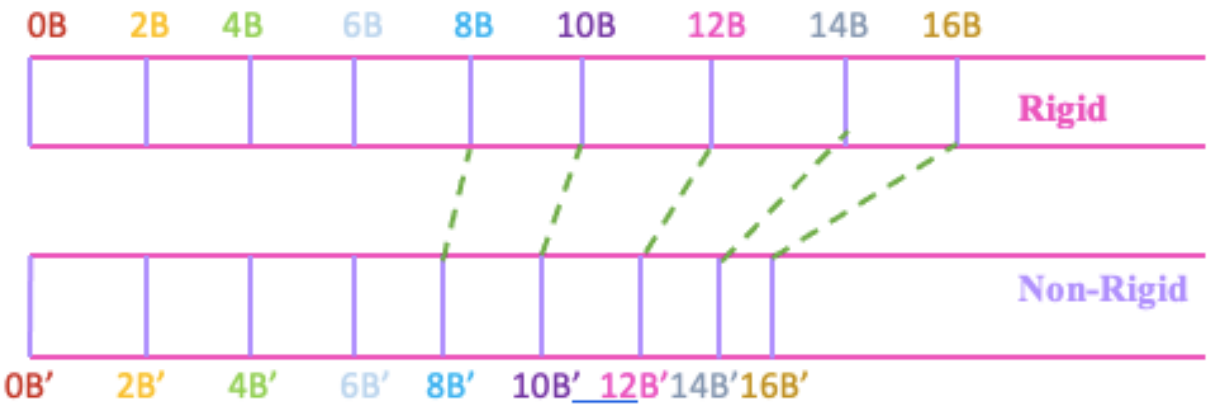

Figure 3. 9: Centrifugal distortion constant effect

Singh, R. (2021). Rigid and non-rigid rotor models for microwave rotational spectroscopy of diatomic molecules. *International Journal of Advanced Science and Engineering*, *7*(4), 1946–1942. https://doi.org/10.29294/ijase.7.4.2021.1936-1942

For symmetric tops, the Hamiltonian for the centrifugal distortion constant expands further and is composed of 2 more parameters, D_{JK} and D_K other than the original D_J. It will be expressed as shown in equation 3.21.

$$H_{\mathrm{BH}} = -D_{\backslash}J^{2} - D_{\backslash\mathrm{c}}J^{2}J_{+} - D_{2}J_{+}^{2} \qquad (3.21)$$

The energy of a symmetric top is divided further based on what type of symmetric top we are going over. Such as the prolate symmetric top that will have proceeding energy seen by equation 3.22.

$$E_{\backslash,\mathrm{c}} = BJ(J+1) + (A-B)K^{"} - D_{\backslash}J^{"}(J+1)^{"} - D_{\backslash\mathrm{c}}J(J+1)K^{"} - D_{\mathrm{c}}K^{4} \quad (3.22)$$

The oblate symmetric non-rigid rotor the energy equation will be seen in equation 3.23

$$E_{\backslash,\mathrm{c}} = 2B(J+1) - 4D_{\backslash}(J+1)^{\mathrm{C}} - 4D_{\backslash\mathrm{c}}(J+1)K^{"} \qquad (3.23)$$

The asymmetric top will have other 2 parameters that need consideration to describe the spectra clearly. These parameters are from Watson's A-reduced form of a distortable rotor by including δ_J and δ_k next to the D_J, D_{JK}, and D_K. An asymmetric top energy for a non-rigid rotor can be seen in equation 3.24

$$E_{\backslash,\mathrm{c}} = 2B(J+1) - 4D_{\backslash}(J+1)^{\mathrm{C}} \qquad (3.24)$$

3.5 Large Amplitude Motions

The large amplitude motions of a molecule is something of our interest that will be explained in this chapter. Since our molecule has a large amplitude motion based on what we have analyzed theoretically and experimentally, we will have to first focus on a harmonic oscillator, a particle in a potential energy well given by force constant (Atkins 2014). This is based on having kinetic energy and potential energy at the non-zero regarding the motion of the ground state. When we have a free particle, the potential energy is zero since there is no force in which we note this being a one-dimensional moving on the x-axis. The energy levels are not being quantized since there is a continuation in the kinetic energy. Thus, this motion is where the particle's position cannot be definite if it moved through the axis. Torsion angle rotations are the most important based on the intramolecular regarding the field of force. Torsion angle interaction tried to model the rotational barriers by combining non-bonded interactions and mostly since it is different regarding the stretching and bending interactions. A torsional potential study was done on toluene, where the torsional potential can also be seen in the spectrum. To get the spectrum from the toluene by different torsional levels that had to be fixed by assuming some torsion-electronic coupling by permitting only one torsional transition to occur (Müller 2017). There were spectra where they could see the torsional levels of a state of toluene from the intermediate resonance how the torsional barrier can affect and this by helping understand the large amplitude motion.

The large amplitude motions are molecular movements that will have large atomic displacements. This is based on the feature produced for specific rotational spectra when certain barriers are within the molecule’s geometry (Wlodarczak 1999). It has been denoted based on various large amplitude motions of molecules rigid models by the motions in rotation from a bond or inversion and bending

of a near-linear molecule (Strauss 1983). This is fundamental to have a stable geometry and small amplitude displacement thus since there will be bonded fixing. Large amplitude motions can be reflected by the molecular movements compromising internal rotations, proton tunneling, and low energy vibrational frequencies (Hakiri 2019). However, these large amplitude motions are difficult to do in quantum calculations that will require a stronger experimental counterpart for the theoretical models since it is based on the rotor of the model's system.

The large amplitude motions of a molecule could be analyzed on different molecules based on the stretching or torsion of the bonds of the molecules from the gas phase microwave spectrum. These then have a potential energy scan based on their stability and energy from their degree of freedom based on their bond, such as the ester of small fruit found on the C–C single bond having a large amplitude motion (Hakiri 2019). Dr. Haikiri and his collaborators could denote in the study that there were different types of four different pentanoates through their gas-phase structure from the intramolecular effect having to use lower optimization to expect some reliable data from the structure. The large amplitude motion had been studied in the spectra stimulation doing potential energy scans of superfluid and non-superfluid to unravel the deformation dynamic and rotation. It can cause regarding being isolated (Briant 2019). This study from Dr. Briant and his collaborators was based on the dynamical effect on the spectrum and denoting the large amplitude motions based on the complex molecule being perturbed regarding the environment.

3.6 CP-FTMW Spectrometer

Chirped-Pulse Fourier Microwave (CP-FTMW) Spectrometer was invented in 2006 and is a microwave spectrometer used today with other spectrometers used for studies. This spectrometer was proposed by Dr. Brook H. Pate and collaborators from the University of Virginia. This CP-FTMW was designed to measure from the spectrum of 7.5 to 18.5 GHz with a single polarizing pulse advancing the digital electronic (Brown 2006). A digital oscilloscope digitally converts the molecule's free induction decay from the time domain by increasing the signal-to-noise ratio. The chirped-pulse microwave spectrometer is a gas phase technique used for pure rotational spectrum for the unambiguous identification of permanent electric dipole moments (Pajski 2008). The Chirped-pulse FTMW spectrometer adds a waveform of generator that expands the bandwidth of several 1000x. The amount of time needed will decrease to undergo a spectral search.

The CP-FTMW was developed to offer the order of magnitude improvement in the spectrum acquisition times and its advantage in digital electronics in measuring the molecular spectrum (Brown 2006). The chirped pulse was created to offer two crucial advantages, such as the frequency bandwidth and pulse duration, which are decoupled in the chirped pulse. Also, the behavior is different from the transform-limited since the pulse is used in a Fourier transform spectroscopy since bandwidth is increasing and must be achieved by shortening the pulse. Thus, by using the "stretched" pulse, it can deliver more energy from the sample from the microwave amplifier with the fixed peak power. Then for a chirped microwave pulse, there is a simpler method in the extension within the bandwidth. So, when the chirped pulse passes through the microwave frequency multiplies, the bandwidth will increase the force by multiplying from the device while the pulse is going to be preserved. The CP-FTMW spectroscopy applies the

isomerization kinetics and the rich dynamics behavior of the geometry reversible reaction. The chirped pulse was designed over the excitation with a linear frequency sweep which was created and amplified. This can be conveyed in the schematic in Figure 3.10 of the CP-FTMW spectrometer that was made for microwave spectroscopy.

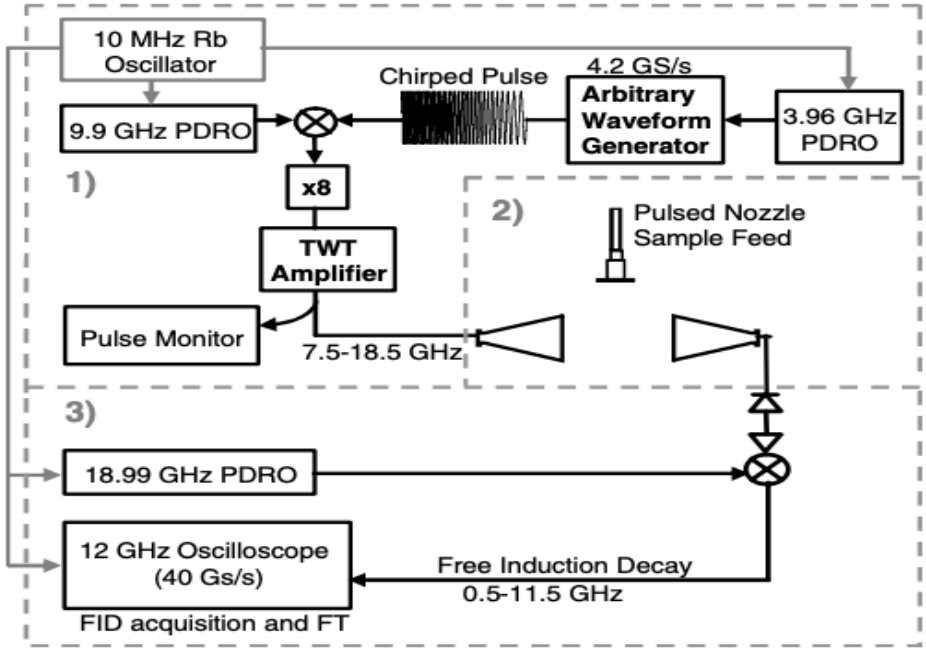

Figure 3. 10: CP-FTMW Spectrometer schematic

Brown, G. G., Dian, B. C., Douglass, K. O., Geyer, S. M., & Pate, B. H. (2006). The rotational spectrum of EPIFLUOROHYDRIN measured by chirped-pulse Fourier transform microwave spectroscopy. *Journal of Molecular Spectroscopy*, *238*(2), 200–212. https://doi.org/10.1016/j.jms.2006.05.003

The CP-FTMW spectrometer schematic diagram shows how the chirped pulse is generated by the high-speed arbitrary waveform generator (AWG) and by a microwave circuit for the frequency up-conversion and a bandwidth extension (Brown 2006). Then the chirped

pulse is amplified by a pulse traveling wave-tube to a linear frequency sweep of .5 to 18.5 GHz in a 1-μs pulse duration. The amplified pulse will be broadcast in a sample interaction region of a molecular-beam spectrometer with a strander gain horn. The molecular beam is created from a pulsed jet expansion of a 0.5% from an 80:20 neon to helium gas mixture. The backing behind the nozzle is about 1 atm, and the pressure nozzle diameter is 1mm, and the pulse duration is 500 μs. The rotational free induction decay is collected by the second horn and is amplified and then converted down from the 0.5 to 11.5 GHz band, and it is digitalized at the 40Gs/s by the digital oscilloscope.

The molecules at their ground-state energy will absorb radiation. They will be more excited, although all the molecules prefer being at the low energy state. After the microwave radiation stops, the molecule will undergo rotational transition, emit the radiation, and return to their ground state. Thus, microwave spectroscopy focuses on the radiation that the molecules have omitted. These signals will be collected for the time domain, and Fourier transformed into the frequency domain. It will allow for an amount of great information that will be collected by a spectrometer and converted into the spectrum for a simple interpretation.

The Chirped-Pulse Fourier transform was used in this research; the experimental work was done at the Missouri University of Science and Technology with Dr. G. Smitty Grubbs and his research group.

CHAPTER VI

ROTATIONAL SPECTROSCOPY NONAFLUORO-TERT-BUTYL ALCOHOL

4.1 Theoretical Work

Our theoretical work for nonafluoro-tert-butyl alcohol (NFTBA) focuses on scanning the potential energy surface to find the most stable conformation and further geometric optimization. There are a total of five central atoms in NFTBA, the four carbon atoms and one oxygen atom. For the four carbon atoms, the local geometries can be estimated to be tetrahedral shape based on the VESPR theory. Their best structures can be obtained by geometry optimization. However, the local structure around the oxygen atom is not a simple geometry optimization since multiple conformations may be possible due to the location of the hydrogen atoms. The alcohol can be stabilized with fluorine and is difficult to optimize with geometry optimization. So, we had to carry out a potential energy scan; from there, we had to mainly go based on the oxygen with the hydrogen it can be stable with the fluorine to optimize the structure. The potential energy scan along the τC1-C2-O14-H15 dihedral angle was performed for this purpose. From chemical intuition, we can estimate that the three CF3 groups are equivalent. From there, we could expect to see three equivalent conformations with the alcohol, making hydrogen bond contact with the fluorine atoms. For our potential energy scan, we did it over the dihedral angle for 36 steps, with each step at 10° at the B3LYP/6-311++G level, to

identify the stable conformations and the energy barriers. The resulting potential energy curve from the scan is shown in Figure 4.1.

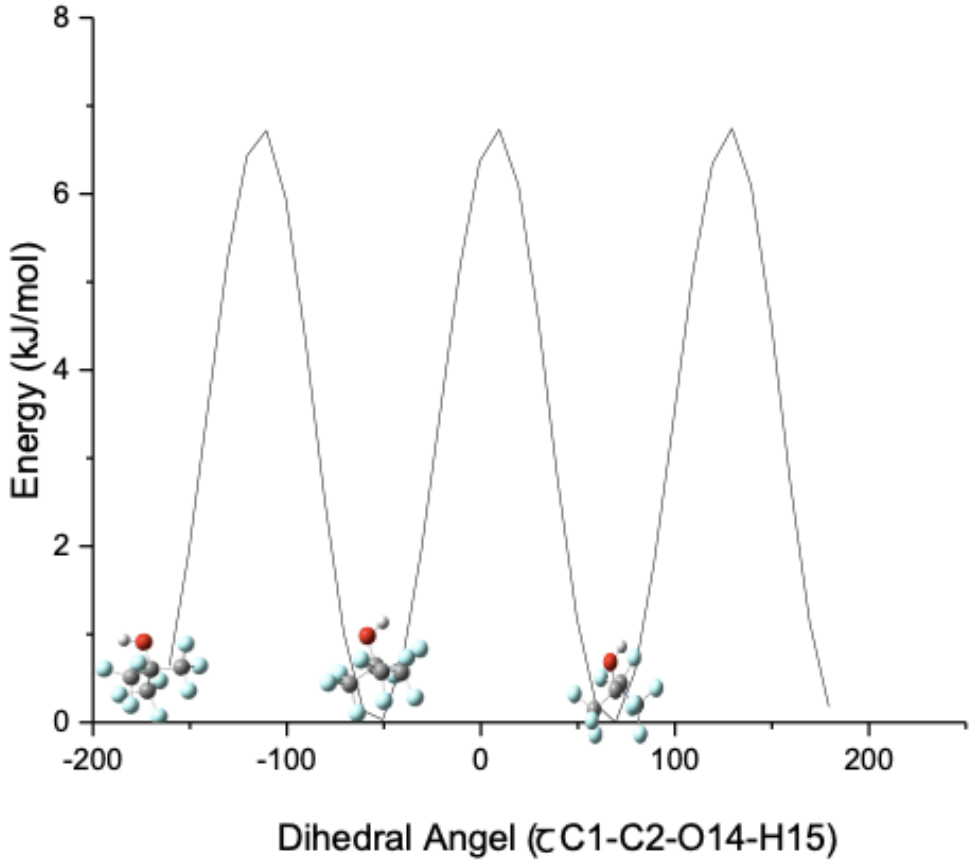

Figure 4. 1: Potential Energy Scan for Nonafluoro-tert-butyl alcohol conformation along with dihedral angle τC1-C2-O14-H15

From the potential energy curve, we can observe that there are indeed three equivalent conformations, as shown in Figure 4.1. In going with this potential energy scan, we could able also see the energy barrier among the lowest confirmation. We can compare the barriers to similar molecules to see if there is a fluorination effect. The energy barrier is about 6.74 kJ/mol. The internal fluorination effect is mostly by the fluorines are equivalent but can cause some barriers based on how they are having with the oxygen some competition for the hydrogen since

fluorine is more electronegative that is caused for our molecule form being an asymmetric molecule to be a near oblate top molecule.

From our overall theoretical work, we had done from our theoretical work from our molecule, then we can also be able to show you how our data overall gave us some insight into how our molecule acts. This also gave us on how our molecule is being done in a potential energy scan we could be able to see the interaction from the bond angles geometry and the energy barriers, and the fluorination effects to compare our molecule with the tert-butyl alcohol in Table 4.1.

Table 4. 1:Energy barriers comparison of NFTBA with TBA

	NFTBA	TBA
kJ/mol	6.74	5.13

Having this energy barrier comparison, we could see the differences on seeing how fluorine makes the energy higher from what was done from their theoretical work. Thus, we can see from table 4.1 is that NFTBA is higher than TBA as explained with the fluorine and by how the structures always prefer the low energy from comparing this data. However, they have a small energy barrier in comparison these two molecules have a large amplitude motion we can still observe how this affects occurs by the fluorine's interacting with the hydrogen.

From the results of the potential energy scan, we were now able to carry out geometric optimization. Since the three lowest energy conformations are equivalent, we could now just focus on one of them for geometry optimization. These further geometric optimizations for NFTBA were conducted using DFT and MP2 with the basis set aug-cc-pVTZ.

The structural parameters from the calculations are compared to the previous electron diffraction work done with perfluoro-tert-butyl alcohol, shown in Table 4.2.

Structural Parameters	DFT/ aug-cc-pVTZ	MP2/ aug-cc-pVTZ	Experimental Electron diffraction
C-C	1.5726A	1.5534A	1.566 ± 0.009 A
C-F	1.3339A	1.3306A	1.335 ± 0.004 A
C-O	1.3928A	1.3919	1.414 ± 0.022 A
∠CCF	111.0^{o}	111.0^{o}	110.6 ± 0.4^{o}
∠CCO	109.3^{o}	109.9^{o}	108.5 ± 0.8^{o}
∠CCC	111.0^{o}	110.2^{o}	110.4 ± 0.8^{o}
∠FCF	108.1^{o}	108.5^{o}	108.3 ± 0.4^{o}

Table 4. 2:Structural Parameters of NFTBA

From what was observed comparing the geometry optimization from our MP2 and DFT, we could compare with the experimental electron diffraction because they are equivalent to each other. In the bond length and angles, we could observe they were close to each other; however, this is based on the large amplitude of motion with the MP2 of the angle,$\angle$CCO, we could observe that it was not exactly that close to what we were observing though the structural parameters.

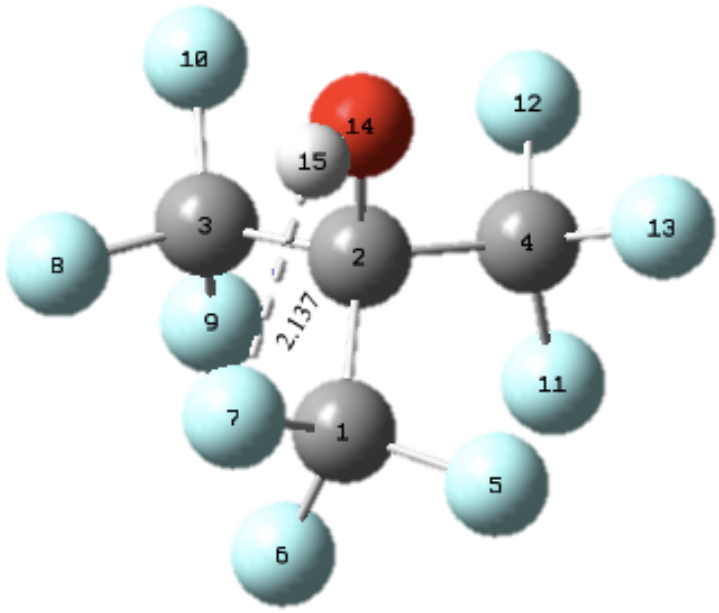

Figure 4. 2: Calculated structure of NFTBA

The Figure 4.2 bond length is perfect to be closed from the hydrogen to the fluorine; the distance between them is 2.137A, as a comparison to the H–F bond, which is 0.91A. Even though the distance from 2.137A is not that close to the covalent bond from H–F shows how fluorine interacts with hydrogen by having the oxygen and fluorine be in competition based on their electronegativity.

4.2 Experimental Work

Based on our calculation from DFT and MP2, we simulate the rotational spectrum of NFTBA to guide our experimental work. These values will be able to provide how we can compare what we have done based on our geometry optimization, being able to see how our

molecule looks based on the fluorine and oxygen from the alcohol haven some stability. This resource we can see from Table 4.3 in which we compare our theoretical work with our experimental work done in collaboration with Dr. Grubbs in the lab in MS&T.

Table 4. 3: Calculations of NFTBA

	B3LYP/ aug-cc-pVTZ	MP2/ aug-cc-pVTZ	Experimental
A (MHz)	805.95	821.81	818.6472(97)
B (MHz)	803.55	820.32	817.2253(10)
C (MHz)	576.39	591.96	591.96(Fixed)
D_J (kHz)			0.03640(57)
D_{JK} (kHz)			0.1010(10)
μ_a (Debye)	1.1	1.2	
μ_b (Debye)	0.0	0.0	
μ_c (Debye)	0.9	1.0	
n*	/	/	16
σ (kHz)[(a)]	/	/	

*n is the number of transitions that are done for experimental work

[(a)]σ is the standard deviation for experimental work

The spectrum of what is determined is based on the represented rotational calculation from the MP2/aug-cc-pVTZ calculations. Figure 4.3 below shows the simulated spectrum from our theoretical work.

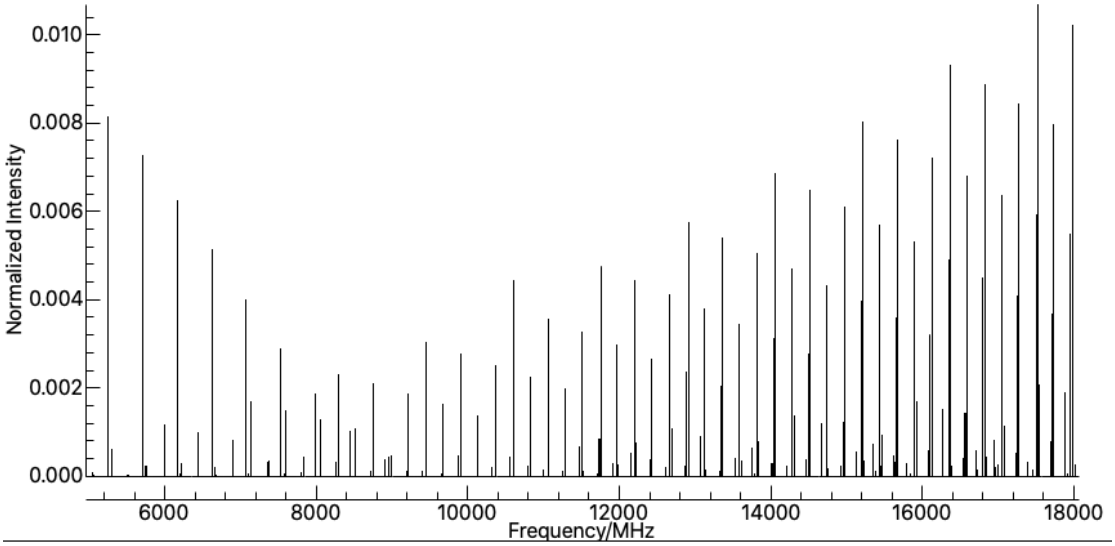

Figure 4. 3: Simulated calculation Nonafluoro-tert-butyl alcohol

Using the calculated rotational constants and dipole moments of nonafluoro-tert-butyl alcohol, the microwave spectrum of nonafluoro-tert-butyl alcohol was simulated using the Pgopher program from our first theoretical work. This spectrum of what is determined is based on the represented rotational calculation from the MP2/aug-cc-pVTZ calculations.

We collaborated with Dr. Grubbs and his research group at the Missouri University of Science and Technology in doing the experimental work. By then, we had our theoretical work. We went and worked on using their lab work to see our molecule's rotational spectrum, and we were able to use their Chirped Pulse FTMW spectrometer to run our sample of nonafluoro-tert-butyl alcohol. We had to ensure the equipment was working well and be careful in using the

software that controlled the chirped pulses. Our sample had to be released along with a carrier gas Aragon. Having followed all the instructions on using the chirped pulses by getting the high vacuum pressure of the spectrum acquisition started. Using a computer program, we could send commands on the CP-FTMW that included the frequency range which we could observe and when to send the microwave signals. The observation was from 5–18 GHz to work getting our spectrum.

For experimental work, we measured the spectrum of nonafluoro-tert- butyl alcohol using the chirped-pulse Fourier transform microwave spectroscopy at Missouri Science and Technology University. Using the calculated rotational constants as a guide, we obtained the preliminary fit from fitting 19 *c*-type transitions. The fitting error is 8.5 kHz, well below the experimental error of the estimated 50 kHz. The C rotational constant was not as well determined. Based on the calculated dipole moments, the spectrum of NFTA features both *a* type and 19 *c* type transitions.

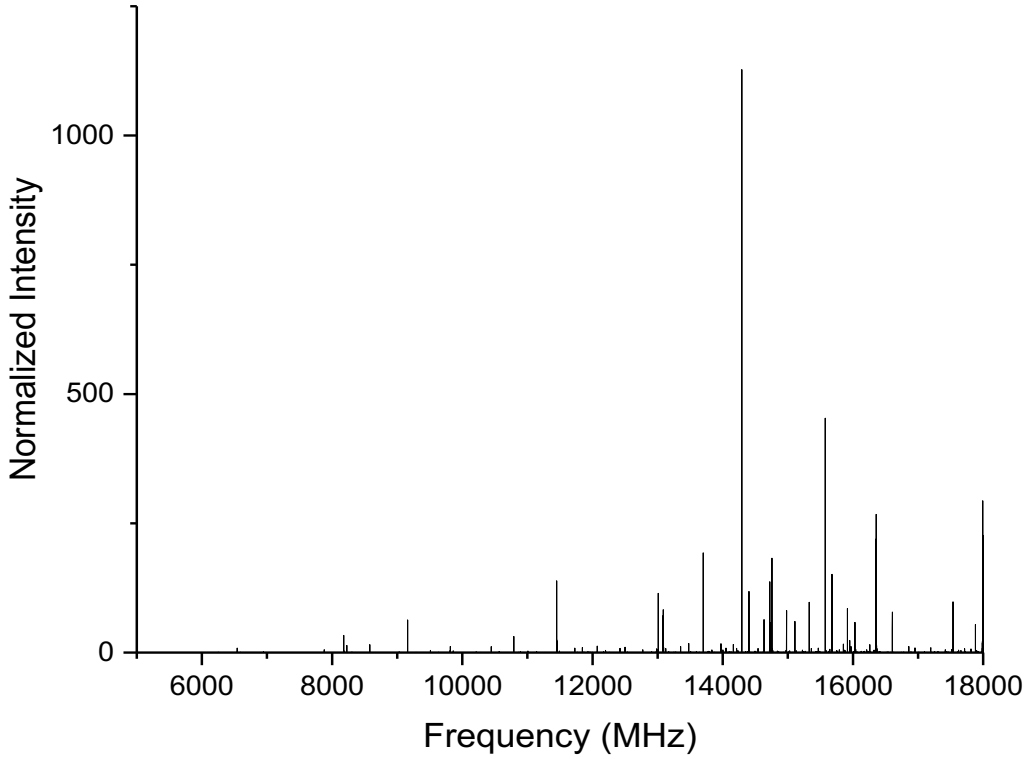

Figure 4. 4: Rotational Spectrum Nonafluoro-tert-butyl alcohol

Based on what we measured in our stimulated and experimental, we were able to compare the distance between our spectrum using our MP2 calculation; the distance between them was around 1635.8 MHz. We measured the spectrum of nonafluoro-tert-butyl alcohol using the chirped-pulse Fourier transform microwave spectroscopy at Missouri Science and Technology University from our experimental and stimulated in Figure 4.4.

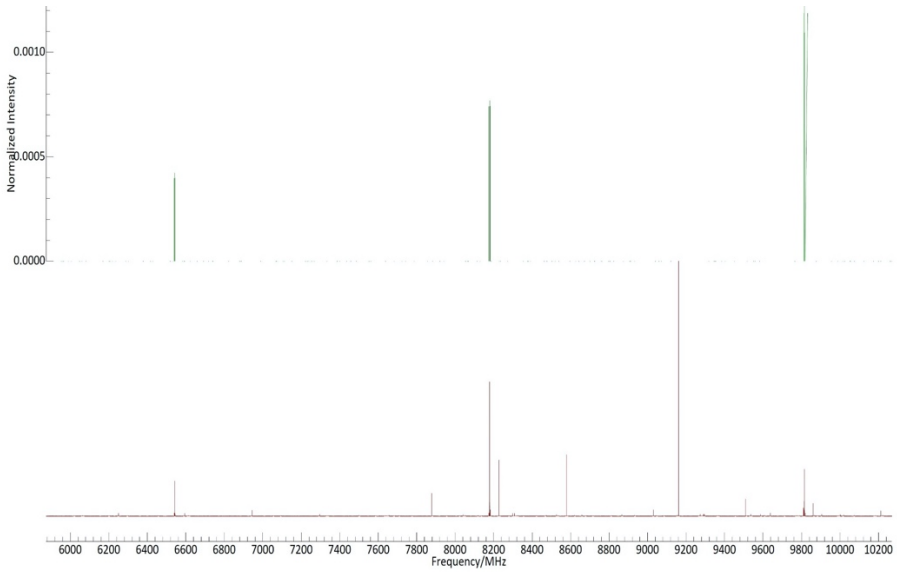

Figure 4. 5: Comparison of experimental (bottom) and simulated *c* type transitions (up) of nonafluoro-tert-butyl alcohol (6 -10 GHz)

We are working on fitting the additional *a* type transitions. The fitted constants are listed in Table 4.4 with the calculated values for comparison. We believe some large amplitude motion based on the hydroxyl group interferes with the rotational energy levels. The two can compare the theoretical values from our collaborators from Dr. Grubbs and our data compared to the experimental, indicating we will need another fitting program to get a complete structure determination from the internal rotation from the O–H group.

Table 4. 4:Preliminary Fitting MS&T and UTRGV

Parameters	MS&T (Error)	Theoretical (MS&T)	UTRGV Fit (Error)
A/ MHz	815.40 (25)	811.50	818.6472(97)
B/MHz	809.63(89)	809.61	817.2253(10)
C/MHz	582.22(87)	582.25	591.96(Fixed)
D_J /kHz	0.03621(24)	/	0.03640(57)
D_{JK}/kHz	0.10199400 (52)	/	0.1010(10)
Transitions	20	/	16
RMS/ MHz	0.926	/	0.008
F_0	597.44486351 (Derived)	570.77	/
V_3/ GHz	1467646532(98)	15225.43707	/

Table 4.4, we can see the comparison in which we have the fitting calculations we have done and MS&T did, and we can see there is not much difference in our calculations. The theoretical MS&T was able to find the three-energy barrier geometry structure and the structure in which they were able to derive. From then, we have to find our structural parameters data for these resources and go further in our investigation now that we have been able to understand that the alcohol caused some large amplitude motions internally from within the molecule, which we are not able to see further within our investigation. In which we were able to see the c-type

transition spectrum from the a-type and b-type. Then by comparing our calculations from the MS&T, we can observe that the root meter square (RMS) is twenty times higher than our RMS since we can observe that they had used the three-energy barrier included within their calculation. Also, when we see their energy barrier that is in GHz is around 5.8 kJ/mol since we can compare that our values are not that away from each other compared to the theoretical. However, this is because of the large amplitude motion from the hydroxyl group that is causing us not to get some accurate data, primarily since we can just determine based on the c-type transitions and we cannot observe other transitions within our data.

4.3 Summary

We measured the first high-resolution rotational spectrum of NFTBA from what we were able to see from our research work.

Our theoretical work for the nonafluoro-tert-butyl alcohol includes Density Functional Theory B3LYP (DFT) and Second-Order Moller-Plesset Perturbation Theory (MP2) using the ab initio calculation method with aug-cc-pVTZ also 6-311++G basis sets. We worked on getting the geometry optimization calculation overall from our molecule using DFT and MP2 with the basis set aug-cc-pVTZ. These calculations were performed through TACC. In that, we have identified NFTBA as a nearly oblate molecule.

Then our overall experimental work was carried out using the Chirped Pulse Fourier microwave transform in the MS&T. The preliminary fit was presented. The final fit was hindered by the large amplitude motion. Further work is needed to clarify the interaction between the large amplitude motion and the rotational energy levels.

REFERENCES

ab-initio calculation. *Oxford Reference.* Retrieved April 12, 2022, from https://www.oxfordreference.com/view/10.1093/oi/authority.20110803095344143.

Ab Initio, Semi-Empirical, and Empirical Force Field Methods. (2019, June 5). Retrieved April 4, 2022, University of Utah. https://chem.libretexts.org/@go/page/70541

Alves, M., Mereau, R., Grignard, B., Detrembleur, C., Jerome, C., & Tassaing, T. (2016). A comprehensive density functional theory study of the key role of fluorination and dual hydrogen bonding in the activation of the epoxide/CO2 coupling by fluorinated alcohols. *RSC Advances*, *6*(43), 36327–36335. https://doi.org/10.1039/c6ra03427f

Becke, A. D., *Phys.* Rev. A, 38, 3098 (1988)

Benioff, P. The computer as a physical system: A microscopic quantum mechanical Hamiltonian model of computers as represented by Turing machines. *J Stat Phys* **22,** 563–591 (1980). https://doi.org/10.1007/BF01011339

Bernath, P. (1995). Spectra of Atoms and Molecules (1st ed.). Oxford University Press

Bernath, P. (2020). Spectra of Atoms and Molecules (4th ed.). Oxford University Press.

Brown, G. G., Dian, B. C., Douglass, K. O., Geyer, S. M., & Pate, B. H. (2006). The rotational spectrum of EPIFLUOROHYDRIN measured by chirped-pulse Fourier transforms microwave spectroscopy. *Journal of Molecular Spectroscopy*, *238*(2), 200–212. https://doi.org/10.1016/j.jms.2006.05.003

Castellan, G. W. (1983). Physical Chemistry (3rd Edition). 503-507

CFOUR, a quantum chemical program package written by J.F. Stanton, J. Gauss, L. Cheng, M.E. Harding, D.A. Matthews, P.G. Szalay with contributions from A. Asthana, A.A. Auer, R.J. Bartlett, U. Benedikt, C. Berger, D.E. Bernholdt, S. Blaschke, Y.J. Bomble, S. Burger, O. Christiansen, D. Datta, F. Engel, R. Faber, J. Greiner, M. Heckert, O. Heun, M. Hilgenberg, C. Huber, T.-C. Jagau, D. Jonsson, J. Jusélius, T. Kirsch, M.-P. Kitsaras, K. Klein, G.M. Kopper, W.J. Lauderdale, F. Lipparini, J. Liu, T. Metzroth, L.A. Mück, T. Nottoli, D.P. O'Neill, J. Oswald, D.R. Price, E. Prochnow, C. Puzzarini, K. Ruud, F. Schiffmann, W. Schwalbach, C. Simmons, S. Stopkowicz, A. Tajti, J. Vázquez, F.

Wang, J.D. Watts, C. Zhang, X. Zheng and the integral packages *MOLECULE* (J. Almlöf and P.R. Taylor), *PROPS* (P.R. Taylor), *ABACUS* (T. Helgaker, H.J. Aa. Jensen, P. Jørgensen, and J.

Olsen), and ECP routines by A. V. Mitin and C. van Wüllen. For the current version, see http://www.cfour.de.

Cline, D. (2020, December 30). *13.6: Principal Axis System*. Physics LibreTexts. Retrieved June 10,2022,https://phys.libretexts.org/Bookshelves/Classical_Mechanics/Variational_Principles_in_ Classical_Mechanics_(Cline)/13%3A_Rigid body_Rotation/13.06%3A_Principal_Axis_System

Cohen, E. A., Drouin, B. J., Valenzuela, E. A., Woods, R. C., Caminati, W., Maris, A., & Melandri, S. (2010). The rotational spectrum of tertiary-butyl alcohol. *Journal of Molecular Spectroscopy*, *260*(1), 77–83. https://doi.org/10.1016/j.jms.2009.11.010

Cooke, S.A., Ohring, P. (2012). Decoding Pure Rotational Molecular Spectra for Asymmetric Molecules. Journal of Spectroscopy, vol. 2013. Article ID 698392, 10 pages. https://doi.org/10.1155/2013/698392

Computer History Museum. Supercomputer designer Seymour Cray in front of his Cray-1 computer. (n.d.). Retrieved May 19, 2022, from https://www.computerhistory.org/revolution/supercomputers/10/7/3

Coomer, J. (1999). *Density Functional Theory for beginners.* Density functional theory for beginners. Retrieved April 8, 2022, from http://newton.ex.ac.uk/research/qsystems/people/coomer/dft_intro.html

Daniel, C. (2021, July 20). *Density functional theories and coordination chemistry*. Comprehensive Coordination Chemistry III (Third Edition) 256-275. Retrieved April 3, 2022, from https://doi.org/10.1016/B978-0-12-409547-2.14828-0

Decato, S., Bemis, T., Madsen, E., & Mecozzi, S. (2014). Synthesis and characterization of perfluoro-tert-butyl semifluorinated amphiphilic polymers and their potential application in hydrophobic drug delivery. *Polym. Chem.*, *5*(22), 6461–6471. https://doi.org/10.1039/c4py00882k

Del Ben, M., Hutter, J., & VandeVondele, J. (2012). Second-order Møller–Plesset perturbation theory in the condensed phase: An efficient and massively parallel Gaussian and plane waves approach. *Journal of Chemical Theory and Computation*, *8*(11), 4177–4188. https://doi.org/10.1021/ct300531w

Deng, J., Gilbert, A. T., & Gill, P. M. (2015). MP2[V]--A Simple Approximation to Second-Order Møller-Plesset Perturbation Theory. *Journal of chemical theory and computation*, 11(4), 1639–1644. https://doi.org/10.1021/acs.jctc.5b00147

Dinoiu, V. (2007). Fluorine chemistry: Past, present and future. *ChemInform*, *38*(44), 1141 1151. https://doi.org/10.1002/chin.200744226

Ditchfield, R; Hehre, W.J; Pople, J. A. (1971). "Self-Consistent Molecular-Orbital Methods. IX. An Extended Gaussian-Type Basis for Molecular-Orbital Studies of Organic Molecules". *J. Chem. Phys*. **54** (2): 724–728. https://doi.org/10.1063/1.1674902.

Dolbier, W. R. (2005). Fluorine chemistry at the millennium. *Journal of Fluorine Chemistry*, *126*(2), 157–163. https://doi.org/10.1016/j.jfluchem.2004.09.033

Dorris, R. E., Trendell, W. C., Peebles, R. A., & Peebles, S. A. (2016). Rotational spectrum, structure, and interaction energy of the trifluoroethylene···Carbon Dioxide Complex. *The Journal of Physical Chemistry A*, *120*(40), 7865–7872. https://doi.org/10.1021 acs.jpca.6b08286

Dunning,T.H., & Hay, P.J.,1977, "Gaussian basis sets for molecular calculations," in: "Modern Theoretical Chemistry," vol. 3. Ed. H.F. Schaefer III, pp. 1-28, Plenum Press, New York.

Dunning, T. H. Jr., 1989, "Gaussian basis sets for use in correlated molecular calculations," J.Chem.Phys. 90, 1007-1023.

Evangelisti, L., & Caminati, W. (2011). A rotational study of the molecular complex tert butanol···1,4-dioxane. *Chemical Physics Letters*, *514*(4-6), 244–246.Filler, R., & Schure, R. M. (1967). Highly acidic perhalogenated alcohols. A new synthesis of perfluoro-tert-butyl alcohol. *The Journal of Organic Chemistry*, *32*(4), 1217–1219. https://doi.org/10.1021/jo01279a081

Fock, V. A. (1930). "Näherungsmethode zur Lösung des quantenmechanischen Mehrkörperproblems". *Z. Phys.* (in German). **61** (1): 126–148. 10.1007/BF01340294

Fock, V. A. (1930). ""Selfconsistent field" mit Austausch für Natrium". *Z. Phys.* (in German). **62** (11): 795–805.10.1007/BF01330439

Foresman, J. B., & Frisch, Æ. (2016). *Exploring chemistry with electronic structure methods* (2nd ed.). Gaussian.

Fuge, R., Andrews, M.J. Fluorine in the UK environment. *Environ Geochem Health* **10,** 96–104 (1988). https://doi.org/10.1007/BF01758677

Gaussian Basis Sets. (2020, March 18). Retrieved April 11, 2022, https://chem.libretexts.org/@go/page/210880

Guo, S., Yang, J., & Liu, Z. (2006). The fate of fluorine and chlorine during thermal treatment of coals. *Environmental Science & Technology*, *40*(24), 7886–7889. https://doi.org/10.1021/es0604562

Gouverneur, V., & Seppelt, K. (2015). Introduction: Fluorine chemistry. *Chemical Reviews*, *115*(2), 563–565. https://doi.org/10.1021/cr500686k

Griller, D., Ingold, K. U., Krusic, P. J., & Fischer, H. (1978). Configuration of the tert-butyl radical. *Journal of the American Chemical Society*, *100*(21), 6750–6752. https://doi.org/10.1021/ja00489a035

H. M. Pickett, "The Fitting and Prediction of Vibration-Rotation Spectra with Spin Interactions," J. Molec. Spectroscopy 148, 371-377 (1991)

H. M. Pickett, R. L. Poynter, E. A. Cohen, M. L. Delitsky, J. C. Pearson, and H. S. P. Muller, "Submillimeter, Millimeter, and Microwave Spectral Line Catalog," J. Quant. Spectrosc. & Rad. Transfer 60, 883-890 (1998)

Han, D. J., Kim, S., Heo, H. J., Park, I. J., Kang, H. S., Lee, S. G., Lee, J.-C., & Sohn, E.-H. (2020). Access to fluorinated polymer surfaces with outstanding mechanical property, high optical transparency, and low surface energy via nonafluoro-tert-butyl group introduction. *ACS Applied Polymer Materials*, *2*(9), 3957–3965. https://doi.org/10.1021 acsapm.0c00625

Han, J., Kiss, L., Mei, H., Remete, A. M., Ponikvar-Svet, M., Sedgwick, D. M., Roman, R., Fustero, S., Moriwaki, H., & Soloshonok, V. A. (2021). Chemical aspects of human and environmental overload with fluorine. *Chemical Reviews*, *121*(8), 4678–4742. https://doi.org/10.1021/acs.chemrev.0c01263

Hanson, D. M., Harvey, E., Sweeney, R., & Zielinski, T. J. (2022, April 12). The Born Oppenheimer Approximation. Retrieved March 31, 2022, from https://chem.libretexts.org/@go/page/1973

Hagmann, W. K. (2008). The many roles for fluorine in medicinal chemistry. *Journal of Medicinal Chemistry*, *51*(15), 4359–4369. https://doi.org/10.1021/jm800219f

Hakiri, R., Derbel, N., Stahl, W., & Mouhib, H. (2019). Large amplitude motions in fruit flavors: The case of alkyl butyrates. *ChemPhysChem*, *21*(1), 20–25. https://doi.org/10.1002/cphc.201900727

Halperns, D. F., & Tatlow, J. C. (1994). Fluorinated Inhalation Anesthetics . *Organofluorine Chemistry*, 543–554. https://doi.org/10.1007/978-1-4899-1202-2_2

Hammersley, J. M., & Handscomb, D. C., "Monte Carlo Methods," Spottiswoode, Ballaantyne & Co. London and Colchester, 1965.

Hanindriyo, A. T., Yadav, A. K., Ichibha, T., Maezono, R., Nakano, K., & Hongo, K. (2022). Diffusion Monte Carlo Evaluation of disiloxane linearisation barrier. *Physical Chemistry Chemical Physics*, *24*(6), 3761–3769. https://doi.org/10.1039/d1cp01471d

Hanson, D. M., Harvey, E., Sweeney, R., & Zielinski, T. J. (2022, April 21). *1: Spectroscopy*. Chemistry LibreTexts. Retrieved June 3, 2022, from https://chem.libretexts.org/Bookshelves/Physical_and_Theoretical_Chemistry_Textbook_Maps/Book%3A_Quantum_States_of_Atoms_and_Molecules_(Zielinksi_et_al)/01%3A_S pectroscopy#:~:text=Spectroscopy%20generally%20is%20defined%20as,%2C%20liquid%2C%20or%20solid%20phase.

Hartree, D.R. (1928) The Wave Mechanics of an Atom with a Non-Coulomb Central Field. Part I. Theory and Methods. Mathematical Proceedings of the Cambridge Philosophical Society, 24, 89-110. http://dx.doi.org/10.1017/S0305004100011919

Hartree, D. R., & W. Hartree, "Self-consistent field, with exchange, for beryllium," Proceedings of the Royal Society of London. Series A - Mathematical and Physical Sciences, vol. 150, no. 869, pp. 9–33, May 1935.

Head-Gordon, M. A. (1993). *Quantum Chemistry Introduction*. Q Chem-Inc. Retrieved February 13, 2022, from https://manual.q-chem.com/4.3/sect-c5Intro.html

Hehre, W. J., W. A. Lathan, R. Ditchfield, M. D. Newton, and J. A. Pople, *Gaussian 70* (Quantum Chemistry Program Exchange, Program No. 237, 1970).

Hill, J.G. and Peterson, K. A. Phys. Chem. Chem. Phys. **12**, 10460 (2010)

Huang, M. (2018). *Spectroscopy Studies of Free Radicals and Ions Containing Large Amplitude Motions* [Doctoral dissertation, Ohio State University]. OhioLINK Electronic Theses and Dissertations Center. http://rave.ohiolink.edu/etdc/view acc_num=osu1515012236254284

Isabel Cabaço, M., Besnard, M., Cruz, C., Morgado, P., Silva, G. M. C., Filipe, E. J. M., Coutinho, J. A. P., & Danten, Y. (2021). The structure of liquid perfluoro tert-butanol using infrared, Raman and X-ray scattering analyzed by quantum DFT calculations and molecular dynamics. *Chemical Physics Letters*, *779*, 138844. https://doi.org/10.1016 j.cplett.2021.138844

Isabel Cabaço, M., Besnard, M., Morgado, P., Filipe, E. J. M., Coutinho, J. A. P., & Danten, Y. (2021). Gaseous hetero dimers of perfluoro tert-butyl alcohol with hydrogenated alcohols by infrared spectroscopy and quantum DFT calculations

Jensen, F. (199AD). *Introduction to computational chemistry*. John Wiley & Sons Ltd.

Jensen, K. F., & Truhlar, D. G. (1987). Supercomputer Research in Chemistry and chemical engineering. *ACS Symposium Series*, 1–14. https://doi.org/10.1021/bk-1987-0353.ch001

Jirak, D., Galisova, A., Kolouchova, K., Babuka, D., & Hruby, M. (2018). Fluorine polymer probes for Magnetic Resonance Imaging: Quo Vadis? *Magnetic Resonance Materials in Physics, Biology and Medicine*, *32*(1), 173–185. https://doi.org/10.1007 s10334-018-0724-6

Kasper, J. J., Hitro, J. E., Fitzgerald, S. R., Schnitter, J. M., Rutowski, J. J., Heck, J. A., & Steinbacher, J. L. (2016). A library of fluorinated electrophiles for chemical tagging and materials synthesis. The Journal of Organic Chemistry, 81(17), 8095–8103. https://doi.org/10.1021/acs.joc.6b01572

Kot, D., Kissinger, G., Schubert, M. A., & Sattler, A. (2017). Current stage of the investigation of the composition of oxygen precipitates in Czochralski silicon wafers. *ECS Journal of Solid State Science and Technology*, *6*(4), 17–24. https://doi.org/10.1149/2.0081704jss

Krishnan, R., Binkley, J. S., Seeger, R., Pople, J. A.Self-consistent molecular orbital methods. XX. A basis set for correlated wave functions J. Chem. *Phys*., 72, 650-654 (1980) 10.1063/1.438955

Lee, C., Yang, W., & Parr, R. G., " Development of the Colle-Salvetti correlation-energy formula into a functional of the lectron density," *Physical Review* B, 37, 785 (1988)

LeGrand, S., Scheinberg, A., Tillack, A. F., Thavappiragasam, M., Vermaas, J. V., Agarwal, R., Larkin, J., Poole, D., Santos-Martins, D., Solis-Vasquez, L., Koch, A., Forli, S., Hernandez, O., Smith, J. C., & Sedova, A. (2020). GPU-accelerated drug discovery with docking on the summit supercomputer. *Proceedings of the 11th ACM International Conference on Bioinformatics, Computational Biology and Health Informatics*. https:/ doi.org/10.1145/3388440.3412472

López-Peacock, E. (1995). Physical Chemistry: A Practical Approach. 115-117.

Lovas FJ. Application of microwave spectroscopy to chemical analysis. ISA Transactions. 1975 ;14(2):145-151. PMID: 1176276.

Lu, T., & Chen, F. (2011). Multiwfn: A multifunctional wavefunction analyzer. *Journal of Computational Chemistry*, *33*(5), 580–592. https://doi.org/10.1002/jcc.22885

Martinez, J.-P. (2016). The hartree-fock method: From self-consistency to correct symmetry. *Annalen Der Physik*, *529*(1-2), 1600328. https://doi.org/10.1002 andp.201600328

McQuarrie, D. A., & Simon, J. D. (1997). *Physical Chemistry: A molecular approach*. University science Books.

Moffitt, W., Ballhausen, C. J. (1956). Quantum Theory. United States: Annual Reviews, Incorporated.

Monroe, C., Meekhof, D. M., King, B. E., & Wineland, D. J. (1996). A "schrödinger cat" superposition state of an atom. *Science*, *272*(5265), 1131–1136. \https://doi.org/10.1126/science.272.5265.1131

Müller-Dethlefs, K., & Ford, M. (2017). Photoelectron Spectroscopy, Zero Kinetic Energy, applications. *Encyclopedia of Spectroscopy and Spectrometry*, 619–627. https://doi.org/10.1016/b978-0-12-803224-4.00252-1

National Aeronautics and Space Administration, Science Mission Directorate. (2010). Introduction to the Electromagnetic Spectrum. Retrieved *June 15, 2022*, from NASA Science website: http://science.nasa.gov/ems/01_intro

NASA. (n.d.). *JPL molecular spectroscopy*. NASA. Retrieved May 23, 2022, from https://spec.jpl.nasa.gov/

National Center for Biotechnology Information (2022). PubChem Element Summary for AtomicNumber 9, Fluorine. Retrieved April 20, 2022 from https://pubchem.ncbi.nlm.nih.gov/element/Fluorine.

National Research Council 1995. *Mathematical Challenges from Theoretical/Computational Chemistry*. Washington, DC: The National Academies Press. https://doi.org/10.17226/4886.

Nejad, A., & Crittenden, D. L. (2020). On the separability of large-amplitude motions in anharmonic frequency calculations. *Physical Chemistry Chemical Physics*, *22*(36), 20588–20601. https://doi.org/10.1039/d0cp03515g

Nesbitt, D. J., & Suhm, M. A. (2010). Chemical Dynamics of large amplitude motion. *Physical Chemistry Chemical Physics*, *12*(29), 8151. https://doi.org/10.1039/c0cp90051f

Newton, G. (2020, November 9). *Fluorine F (element 9) of periodic table - elements flash cards*. NewtonDesk. Retrieved February 18, 2022, from https://www.newtondesk.com/fluorine element/

Our People | Gaussian.com. (n.d.). Gaussian.com. Retrieved April 11, 2022, from https://gaussian.com/people/

Ottaviani, P., Caminati, W., Favero, L. B., Blanco, S., López, J. C., & Alonso, J. L. (2006). Molecular beam rotational spectrum of cyclobutanone-trifluoromethane: Nature of weak ch···o□c and ch···f hydrogen bonds. *Chemistry - A European Journal*, *12*(3), 915–920. https://doi.org/10.1002/chem.200500674

PAJSKI, J. A. S. O. N. J., LOGAN, M. A. T. T. H. E. W. D., DOUGLASS, K. E. V. I. N. O., BROWN, G. O. R. D. O. N. G., DIAN, B. R. I. A. N. C., PATE, B. R. O. O. K. S. H., & SUENRAM, R. I. C. H. A. R. D. D. (2008). Chirped-pulse Fourier transform microwave spectroscopy: A new technique for rapid identification of chemical agents. *International Journal of High Speed Electronics and Systems*, *18*(01), 31–45. https://doi.org/10.1142/s0129156408005114

Park, G. B., & Field, R. W. (2016). Perspective: The first ten years of broadband chirped pulse Fourier transform microwave spectroscopy. *The Journal of Chemical Physics*, *144*(20), 200901. https://doi.org/10.1063/1.4952762

Parra, R. D., & Zeng, X. C. (1998). Rotational barrier for 1,1-difluoroethane, 1,1,1,2 Tetrafluoroethane, pentafluoroethane, and hexafluoroethane: A density functional and ab initio molecular orbital study. *The Journal of Physical Chemistry A*, *102*(3), 654–658. https://doi.org/10.1021/jp972893w

Particle in a 3-Dimensional box. (2019, April 11). Retrieved April 2, 2022, from https://chem.libretexts.org/@go/page/1726

Pavlik, F. J., & Toren, P. E. (1970). Perfluoro-tert-butyl alcohol and its esters. *The Journal of Organic Chemistry*, *35*(6), 2054–2056. https://doi.org/10.1021/jo00831a089

Peterson, K. Gaussian basis sets for molecular calculations (correlation consistent basis sets). http://tyr0.chem.wsu.edu/~kipeters/Pages/ccbasis.html

Physical properties and uses of fluorite. Physical Properties and Uses of Fluorite_Chemicalbook. (2009, December 3). Retrieved February 18, 2022, from https://www.chemicalbook.com/Article/Physical-Properties-and-Uses-of-Fluorite.htm

Programme, U. N. E., Organization, W. H., & Organization, I. L. (1984, January 1). *Fluorine and fluorides - environmental health criteria 36*. UN Environment Document Repository Home. Retrieved Januart 18, 2022, from https://stg-wedocs.unep.org handle/20.500.11822/29338

Reinisch, G., Miki, K., Vignoles, G. L., Wong, B. M., & Simmons, C. S. (2012). An efficient and accurate formalism for the treatment of large amplitude intramolecular motion. *Journal of Chemical Theory and Computation*, *8*(8), 2713–2724. https://doi.org/10.1021 ct300278x

Roesky, H. W. (2010). A flourish of fluorine. *Nature Chemistry*, *2*(3), 240–240. https://doi.org/10.1038/nchem.569

Sack, H. (2021, October 31). *John A. Pople and computational methods in quantum chemistry*. SciHi Blog. Retrieved February 12, 2022, from http://scihi.org/john-pople computational-quantum-chemistry/

Scheirs, J. (1997). *Modern fluoropolymers: High performance polymers for diverse applications*. Wiley.

Schrödinger, E. (n.d.). *English translation from: E. Schrödinger (1982): Collected papers on ...* Retrieved April 25, 2022, from http://people.isy.liu.se/jalar/kurser/QF/references/Schrodinger1926b.pdf

Schmitt, M., Meerts, L. (2018). Structures and Dipole Moments of Molecules in Their Electronically Excited States. Frontiers and Advances in Molecular Spectroscopy, 143-193.

Service, R. F. (2016, June 20). *China overtakes U.S. supercomputing lead | science | AAAS*. https://www.science.org/content/article/china-overtakes-us-supercomputing-lead. Retrieved August 16, 2022, from https://www.science.org/content/article/china-overtakes-us-supercomputing-lead

Sherrill, D. C. (2000). An Introduction to Hartree-Fock Molecular Orbital Theory. http://vergil.chemistry.gatech.edu/notes/hf-intro/hf-intro.pdf

Sherry, A. D., & Purcell, K. F. (1972). Linear enthalpy-spectral shift correlation for perfluoro tert-butyl alcohol. *Journal of the American Chemical Society*, *94*(6), 1853–1857. https://doi.org/10.1021/ja00761a011

Silbey, R., Alberty, R., Bawendi, M. (2005). Physical Chemistry (4th Edition). 329-331.

Silbey, R., Alberty, R., Bawendi, M. (2005). Physical Chemistry (4th Edition). 397-398.

Singh, G., Kumari, B., Sinam, G., Kriti, Kumar, N., & Mallick, S. (2018). Fluoride distribution and contamination in the water, soil and plants continuum and its remedial technologies, an Indian perspective– A Review. *Environmental Pollution*, *239*, 95–108. https://doi.org/10.1016/j.envpol.2018.04.002

Singh, R. (2021). Rigid and non-rigid rotor models for microwave rotational spectroscopy of diatomic molecules. *International Journal of Advanced Science and Engineering*, *7*(4), 1946–1942. https://doi.org/10.29294/ijase.7.4.2021.1936-1942

Spada, L., Tasinato, N., Bosi, G., Vazart, F., Barone, V., & Puzzarini, C. (2017). On the competition between weak O H···F and C H···F hydrogen bonds, in cooperation with C H···O contacts, in the difluoromethane – tert-butyl alcohol cluster. *Journal of Molecular Spectroscopy*, *337*, 90–95. https://doi.org/10.1016/j.jms.2017.04.001

Stephens, P. J., Devlin, F. J., Chabalowski, C. F., & Frisch, M. J. (1994). Ab initio calculation of vibrational absorption and circular dichroism spectra using density functional force fields. *The Journal of Physical Chemistry*, *98*(45), 11623–11627. https://doi.org/10.1021/j100096a001

Strauss, H. L. (1983). Pseudorotation: A large amplitude molecular motion. *Annual Review of Physical Chemistry*, *34*(1), 301–328. https://doi.org/10.1146/annurev.pc.34.100183.001505

Strinati, G.C. (2005). Hartree and Hartree-Fock Methods in Electronic Structure. Encyclopedia of Condensed Matter Physics, 311-318.

Struve, W. S. (1989). Fundamentals of Molecular Spectroscopy. 83-87.

Szabo, A., Ostlund, N.,(1996). Modern Quantum Chemistry Introduction to Advanced Electronic Structure Theory. Dover Publications Inc.

Tanabe, K., Harada, H., Narazaki, M., Tanaka, K., Inafuku, K., Komatsu, H., Ito, T., Yamada, H., Chujo, Y., Matsuda, T., Hiraoka, M., & Nishimoto, S.-ichi. (2009). Monitoring of biological one-electron reduction by 19f NMR using hypoxia selective activation of an 19F-labeled Indolequinone derivative. Journal of the American Chemical Society, 131(44), 15982–15983. https://doi.org/10.1021/ja904953b

Texas Advanced Computing Center. Texas Advanced Computing Center. (n.d.). Retrieved April 6, 2022, from https://www.tacc.utexas.edu/

Thakkar, A. (2014). Quantum Chemistry. 6-1-6-5.

The Energy Levels of a Rigid Rotor. (2021, October 20). https://chem.libretexts.org/@go/page/13422

The Selection Rule for the Rigid Rotor. (2021, May 11). Retrieved April 28, 2022, from https://chem.libretexts.org/@go/page/13675

Thomas, J., & Xu, Y. (2014). Structure and tunneling dynamics in a model system of peptide co solvents: Rotational spectroscopy of the 2,2,2-trifluoroethanol···water complex. *The Journal of Chemical Physics*, *140*(23), 234307–1-234307–5. https://doi.org/10.1063/1.4883518

Thomas, J., Peña, I., Carlson, C. D., Yang, Y., Jäger, W., & Xu, Y. (2020). Structural and dynamical features of the 2,2,2-trifluoroethanol···ammonia complex. *Physical Chemistry Chemical Physics*, *22*(40), 23019–23027. https://doi.org/10.1039/d0cp03329d

Thomas, J., Seifert, N. A., Jäger, W., & Xu, Y. (2017). A direct link from the gas to the condensed phase: A rotational spectroscopic study of 2,2,2-Trifluoroethanol trimers. *Angewandte Chemie International Edition*, *56*(22), 6289–6293. https://doi.org/10.1002anie.201612161

Townes, C.H., Schawlow, A.L. (1955). Microwave Spectroscopy Dover Publication Inc. 2012.

Tressler, C. M., & Zondlo, N. J. (2016). Synthesis of perfluoro-tert-butyl tyrosine, for application in 19F NMR, via a diazonium-coupling reaction. *Organic Letters*, *18*(24), 6240–6243. https://doi.org/10.1021/acs.orglett.6b02858

Valenzuela, E. A. (1975). *Internal Rotation In Heavy Top Molecules: The Microwave Spectrum Of Tertiary-butyl Alcohol And Tertiary-butyl Mercaptan* (Order No. 7520796). Available from ProQuest Dissertations & Theses Global. (302751650). Retrieved from https://go.openathens.net/redirector/utrgv.edu?url=https://www.proquest.com dissertations-theses/internal-rotation-heavy-top-molecules-microwave docview/302751650/se-2?accountid=7119

van Mourik T, Bühl M, Gaigeot MP. Density functional theory across chemistry, physics and biology. *Philos Trans A Math Phys Eng Sci*. 2014;372(2011):20120488. Published 2014 Feb 10. doi:10.1098/rsta.2012.0488

von Neumann, J., and E. Wigner, 1929, *Phys*. Z. 30:465.

Walker, M. C., Thuronyi, B. W., Charkoudian, L. K., Lowry, B., Khosla, C., & Chang, M. C. (2013). Expanding the fluorine chemistry of living systems using engineered polyketide synthase pathways. *Science (New York, N.Y.)*, *341*(6150), 1089–1094. https://doi.org/10.1126/science.1242345

Wakselman, C., & Lantz, A. (1994). Perfluoroalkyl bromides and Iodides. *Organofluorine Chemistry: Principles and Commercial Applications*, 177–194. https:/ doi.org/10.1007/978-1-4899-1202-2_8

Western, C. M. (2017). PGOPHER: A program for simulating rotational, vibrational, and electronic spectra. *Journal of Quantitative Spectroscopy and Radiative Transfer*, *186*, 221–242. https://doi.org/10.1016/j.jqsrt.2016.04.010

Wilson, E. B. (1968). Microwave Spectroscopy in Chemistry. *Science*, *162*(3849), 59–66. http:/ www.jstor.org/stable/1725463

Wlodarczak, G. (1999). Microwave and radiowave spectroscopy, applications*. *Encyclopedia of Spectroscopy and Spectrometry*, 1527–1536. https://doi.org/10.1016 b978-0-12-374413-5.00203-7

Wu, T., Li, A., Chen, K., Peng, X., Zhang, J., Jiang, M., Chen, S., Zheng, X., Zhou, X., & Jiang, Z.-X. (2021). Perfluoro-tert-butanol: A cornerstone for high performance fluorine-19 magnetic resonance imaging. *Chemical Communications*, *57*(63), 7743–7757. https://doi.org/10.1039/d1cc02133h

Y. Shao, Z. Gan, E. Epifanovsky, A. T. B. Gilbert, M. Wormit, J. Kussmann, A. W. Lange, A. Behn, J. Deng, X. Feng, D. Ghosh, M. Goldey P. R. Horn, L. D. Jacobson, I. Kaliman, R. Z. Khaliullin, T. Kús, A. Landau, J. Liu, E. I. Proynov, Y. M. Rhee, R. M. Richard, M. A. Rohrdanz, R. P. Steele, E. J. Sundstrom, H. L. Woodcock III, P. M. Zimmerman, D. Zuev, B. Albrecht, E. Alguire, B. Austin, G. J. O. Beran, Y. A. Bernard, E. Berquist, K. Brandhorst, K. B. Bravaya, S. T. Brown, D. Casanova, C.-M. Chang, Y. Chen, S. H. Chien, K. D. Closser, D. L. Crittenden, M. Diedenhofen, R. A. DiStasio Jr., H. Dop, A. D. Dutoi, R. G. Edgar, S. Fatehi, L. Fusti-Molnar, A. Ghysels, A. Golubeva-Zadorozhnaya, J. Gomes, M. W. D. Hanson-Heine, P. H. P. Harbach, A. W. Hauser, E. G. Hohenstein, Z. C. Holden, T.-C. Jagau, H. Ji, B. Kaduk, K. Khistyaev, J. Kim, J. Kim, R. A. King, P. Klunzinger, D. Kosenkov, T. Kowalczyk, C. M. Krauter, K. U. Lao, A. Laurent, K. V. Lawler, S. V. Levchenko, C. Y. Lin, F. Liu, E. Livshits, R. C. Lochan, A. Luenser, P. Manohar, S. F. Manzer, S.-P. Mao, N. Mardirossian, A. V. Marenich, S. A. Maurer, N. J. Mayhall, C. M. Oana, R. Olivares-Amaya,D. P. O'Neill, J. A. Parkhill, T. M. Perrine, R. Peverati, P. A. Pieniazek, A. Prociuk, D. R. Rehn, E. Rosta, N. J. Russ, N. Sergueev, S. M. Sharada, S. Sharmaa, D. W. Small, A. Sodt, T. Stein, D. Stück, Y.-C. Su, A. J. W. Thom, T. Tsuchimochi, L. Vogt, O. Vydrov, T. Wang, M. A. Watson, J. Wenzel, A. White, C. F. Williams, V. Vanovschi, S. Yeganeh, S. R. Yost, Z.-Q. You, I. Y. Zhang, X. Zhang, Y. Zhou, B. R. Brooks, G. K. L. Chan, D. M. Chipman, C. J. Cramer, W. A. Goddard III, M. S. Gordon, W. J. Hehre, A. Klamt, H. F. Schaefer III, M. W. Schmidt, C. D. Sherrill, D. G. Truhlar, A. Warshel, X. Xua, A. Aspuru-Guzik, R. Baer, A. T. Bell, N. A. Besley, J.-D. Chai, A. Dreuw, B. D. Dunietz, T. R. Furlani, S. R. Gwaltney, C.-P. Hsu, Y. Jung, J. Kong, D. S. Lambrecht, W. Liang, C. Ochsenfeld, V. A. Rassolov, L. V. Slipchenko, J. E. Subotnik, T. Van Voorhis, J. M. Herbert, A. I. Krylov, P. M. W. Gill, and M. Head-Gordon. Advances in molecular quantum chemistry contained in the Q-Chem 4 program package.

Yokozeki, A., & Bauer, S. H. (1975). Electron diffraction study of perfluoro-tert-butyl alcohol. large amplitude motions and structure. *The Journal of Physical Chemistry*, *79*(2), 155 162. https://doi.org/10.1021/j100569a013

Yonker, C. R., Wallen, S. L., Palmer, B. J., & Garrett, B. C. (1997). Effects of pressure and temperature on the dynamics of liquid tert-butyl alcohol. *The Journal of Physical Chemistry A*, *101*(50), 9564–9570. https://doi.org/10.1021/jp972154f

Young, D. 2001.The Absolute Beginners Guide to Gaussian. http://www.ccl.net/cca/documents/dyoung/topics-orig/contents.html

Zhou, Y., Peng, L., & Huang, Y. (2018). Duhamel's formula for time-fractional Schrödinger equations. *Mathematical Methods in the Applied Sciences*, *41*(17), 8345–8349. https://doi.org/10.1002/mma.5222

Zielinski, T. J., Harvey, E., Sweeney, R., & Hanson, D. M. (2005). Quantum states of atoms and molecules. *Journal of Chemical Education*, *82*(12), 1880. https://doi.org/10.1021 ed082p1880.2

BIOGRAPHICAL SKETCH

Zayra Leticia Gonzalez was born in Brownsville, Texas; all her life, she studied in Brownsville from Russel Elementary to her middle school Stell Middle School. She obtained her high school diploma from James Pace High School in December 2014. While she was studying, her brother had Leukemia and passed away, which significantly affected her studies, making her fail for a year. Zayra never stopped working hard; she had been in ballet, karate, and book club from childhood to adolescence. She immediately went the next year and got her basic college core classes at Texas Southmost College until she finished in May 2017. She then transferred and studied at the University of Texas at Rio Grande Valley (UTRGV) to obtain her bachelor's degree in Chemistry in December 2020. While studying, she did her environmental and physical chemistry research and went to three virtual symposiums ESA2, ABRCMS, and COS, before graduating and in school. After she graduated, she immediately went to study, with the support of her parents; without any break from college, she went straight to obtain her Master's in Chemistry from UTRGV in August 2022. To contact Zayra, her email: zayra.gon9495@gmail.com